Marine Environmental Science (M. Sc.)

MASTER THESIS

Clock gene expression patterns in brain and eyestalk tissue of freshly caught Antarctic krill, *Euphausia superba*, during winter.

Submitted by: CONSTANZE BARK

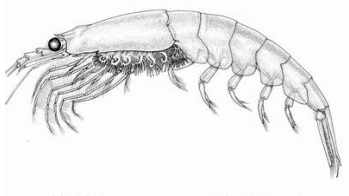

PRINCIPAL SUPERVISOR: Prof Dr Bettina Meyer, University of Oldenburg
CO-SUPERVISOR: Dr Kim Last, Scottish Association for Marine Science

Oldenburg, September 9, 2019

MASTER-THESIS

Clock gene expression patterns in brain and eyestalk tissue of freshly caught Antarctic krill, *Euphausia superba*, during winter

Submitted: September 9, 2019

SUBMITTED BY

Constanze Bark
Matriculation number: 3261087
Am Dobben 35
28203 Bremen
constanze.bark@uni-oldenburg.de

PRINCIPAL SUPERVISOR

Prof Dr Bettina Meyer

Helmholtz Institute for Functional Marine Biodiversity at the University of Oldenburg (HIFMB)
Section: Biodiversity and biological processes in polar oceans
Ammerländer Heerstraße 231, 26129 Oldenburg

Alfred Wegener Institute for Polar- and Marine Research
Section: Polar biological oceanography
Am Handelshafen 12, 27570 Bremerhaven

CO-SUPERVISOR

Dr Kim Last

Scottish Association for Marine Science (SAMS)
Scottish Marine Institute
Oban, Argyll, PA37 1QA

Abstract

The high-latitude Antarctic krill, *Euphausia superba*, is a key species in the Southern Ocean, a region with extreme seasonal and daily changes in photoperiod (day length), light intensity, sea-ice extent, and food availability. In particular, changes in environmental light regimes have been shown to strongly influence krill circadian clock mechanisms and, by extension, synchronized metabolic or physiological output functions. However, knowledge of clock gene functions and regulations in Antarctic krill is still limited, especially with regard to clock gene products, their distribution, and their impact on oscillatory rhythmicity and chronobiological functions. In particular, it is still unclear whether or not the circadian clock might be functioning in krill during summer and winter, when due to the high latitude krill are exposed to near constant light and near constant darkness respectively. This study aims to provide a first basic insight into clock gene expression in wild Antarctic krill during winter conditions. Besides, methodological optimization was attempted to identify putative tissue-specific rhythmic gene expression patterns in brain and eyestalks. In summary, significant 24 h and 16 h oscillatory rhythms could be identified in the relative gene expression of three important clock genes, *Cyc*, *Sgg*, and *Tim*, as well as in the metabolic gene *Atpg* in both krill brain and eyestalks. Additionally, nine of ten tested clock genes displayed a general tendency for upregulation in the early night in both tissues during low to even absent light regime. The results of the present study suggest that krill brain and eyestalks are equally important for clock gene expression due to similar detected amplitudes and therefore the analysis of whole krill heads is recommended for further studies. Furthermore, the results suggest that the circadian clock might be still active in wild krill during winter, despite the extremely low levels of day light to which the animals might be exposed. Future investigations concerning the regulation of endogenous timing systems and rhythmic functions in Antarctic krill might help to understand how circadian functions might be preserved during summer and winter at high latitudes and also how these might be affected by potential environmental alternations driven by climate change.

Key words: Antarctic krill *Euphausia superba*, circadian clock, clock genes, brain and eyestalks, field samples, Bransfield Strait, austral winter, relative mRNA level

Zusammenfassung

Der in hohen Breiten vorkommende Antarktische Krill, *Euphausia superba*, ist eine Schlüsselart im Südpolarmeer, einer Region mit extremen saisonalen und täglichen Veränderungen der Photoperiode (Tageslänge), Lichtintensität, Meereisausdehnung und Nahrungsverfügbarkeit. Es wurde gezeigt, dass Änderungen des Umgebungslichtregimes die zirkadianen Uhr-Mechanismen von Krill und damit auch die synchronisierten metabolischen oder physiologischen Ausgangsfunktionen stark beeinflussen. Jedoch ist das Wissen über die Funktion und Regulation von Uhr-Genen im antarktischen Krill nach wie vor begrenzt, besonders in Bezug auf Uhr-Genprodukte, deren Verteilung und deren Auswirkung auf die oszillatorische Rhythmik und die chronobiologischen Funktionen. Noch ist unklar, ob die zirkadiane Uhr im Sommer und Winter im Krill funktioniert, wenn Krill aufgrund des hohen Breitengrades nahezu konstantem Licht bzw. nahezu konstanter Dunkelheit ausgesetzt ist. Diese Studie soll einen ersten grundlegenden Einblick in die Uhr-Genexpression in wildem antarktischem Krill unter winterlichen Bedingungen geben. Außerdem wurde eine methodische Optimierung getestet, um mutmaßliche gewebespezifische, rhythmische Genexpressionsmuster in Gehirn und Augen zu identifizieren. Zusammenfassend konnten signifikante 24-h- und 16-h-Oszillationsrhythmen in der relativen Genexpression von drei wichtigen Uhr-Genen *Cyc*, *Sgg* und *Tim*, sowie im metabolischen Gen *Atpg* im Gehirn und in Augenstielen des Krills identifiziert werden. Zusätzlich zeigten neun von zehn getesteten Uhr-Genen eine allgemeine Tendenz zur Hochregulation in der frühen Nacht in beiden Geweben, bei schwachem bis sogar fehlendem Lichtregime. Die Ergebnisse der vorliegenden Studie legen nahe, dass das Gehirn und die Augenstiele von Krill aufgrund ähnlicher detektierter Amplituden für die Genexpression von Uhr-Genen gleichermaßen wichtig sind, weshalb die Analyse ganzer Krillköpfe für zukünftige Studien empfohlen wird. Weiterhin deuten die Ergebnisse darauf hin, dass die zirkadiane Uhr im Winter in wildem Krill möglicherweise noch aktiv ist, obwohl das Tageslicht, dem die Tiere ausgesetzt sein könnten, extrem niedrig ist. Zukünftige Untersuchungen zur Regulation endogener Zeitsteuerungssysteme und rhythmischer Funktionen im antarktischen Krill könnten Aufschluss darüber geben, wie zirkadiane Funktionen im Sommer und Winter in hohen Breiten erhalten bleiben und wie diese durch potentielle klimabedingte Umweltänderungen beeinflusst werden können.

Schlüsselwörter: Antarktischer Krill *Euphausia superba*, innere Uhr, Uhr-Gene, Gehirn und Augenstiele, Feldproben, Bransfieldstraße, südlicher Winter, relatives mRNA Level

Index

1 INTRODUCTION 1

1.1 The Antarctic krill *Euphausia superba* 1

1.2 Rhythmic functions in the Antarctic krill, *Euphausia superba* 2

1.2.1 Daily rhythms in krill: diel vertical migration (DVM) 2

1.2.2 Seasonal cycles in krill 4

1.3 Daily biological processes in organisms are regulated by endogenous clocks 5

1.3.1 The circadian clock regulating biological processes 5

1.3.2 The circadian clock on a molecular level using the example of *Drosophila* 6

1.3.3 The circadian clock in marine organisms 8

1.4 The circadian clock in *Euphausia superba*, and mechanisms of regulation 9

1.5 Challenges to circadian regulation in high-latitude species 11

1.6 Aim of study 12

2 MATERIAL & METHODS 13

2.1. Time-series sampling of *E. superba* in the field 13

2.2 Average integrated chlorophyll *a* determination and water temperatures 14

2.3 Irradiance at fishing depth and sea-ice concentration data 15

2.4 Selecting and processing of *E. superba* 16

2.4.1 Tissue separation and processing 16

2.4.2 Dissection of eyestalk and brain tissue 17

2.5 RNA extraction 18

2.6 Preparation of spike controls 21

2.6.1 Transcription of the spikes, purification, and quality control 21

2.6.2 Determination of optimal spike concentration for further chronobiologic analyses 23

2.7 cDNA synthesis of tissue-specific RNA extracts 24

2.8 Analysis of gene expression via TaqMan™ qPCR 24

2.8.1 Custom TaqMan™ Array Card Design 24
2.8.2 Gene selection for the Custom TaqMan™ Array Card 25
2.8.3 Primer design and sequence validation for Custom TaqMan™ Array Card 27
2.8.4 Primer efficiency for all primer sets (in particular for *timeless* and *clock)* 27
2.8.5 qPCR with Custom TaqMan™ Array Cards 29
2.8.6 Data quality control of TaqMan™ qPCR results 29
2.9 Normalization of raw Ct values and relative quantification of mRNAs ... 29
2.10 Statistics 30
3 RESULTS 32
3.1 Regulatory network of clock gene expression patterns 32
3.2 Daily profiles of clock gene expression in brain and eyestalks 33
3.2.1 Analyzed differences within brain and eyestalks tissues 33
3.2.2 Analyzed differences between brain and eyestalks tissue 36
4 DISCUSSION 39
4.1 Environmental conditions in the field 39
Light conditions at fishing depth 39
Krill abundance and chl *a* concentration 40
4.2 Regulation of clock genes in *E. superba* during winter conditions 40
4.3 Comparison of clock gene expression levels in brain and eyestalk tissue 43
Putative co-regulation of clock genes between tissues 44
4.4 Improvements and indications for future studies 46
5 CONCLUSION 48
6 OUTLOOK 49
7 ACKNOWLEDGMENTS 51
8 APPENDIX 52
REFERENCES 56
STATUTORY DECLARATION 63

List of figures

Figure 1: Hypothetical molecular mechnisms of the insect circadian clock in the model organism *Drosophila melanogaster* – The principal auto regulative feedback loop consists of the transcription factors CLOCK (CLK) and CYCLE (CYC), and the regulators PERIOD (PER) and TIMELESS (TIM). In *Drosophila,* CHRYPTOCHROME (CRY1) displays a negative regulator and degrades TIM in a light-dependent manner to reset the clock's phase. CHRYPTOCHROME (CRY2) as an additional negative regulator is not present in Drosophila, but in other arthropods species including the monarch butterfly *Danaus plexippus* (Zhu *et al*., 2008; Merlin *et al*., 2009) and the Antarctic krill (Biscontin *et al*., 2017). SHAGGY (SGG) and DOUBLETIME (DBT) regulate the timing of nuclear entry of TIM and PER by phosphorylating both proteins, respectively. In an additional loop, CLK is cyclically expressed by VRILLE (VRI) and PAR DOMAIN PROTEIN 1ε (PAR1ε), while expression of CYC is still unknown in *Drosophila*, but proposed to be expressed by HR3 and E75 in other insects. In a second additional loop, CLOCKWORK ORANGE (CWO) is rhythmically expressed. Solid lines indicate pathways known for *Drosophila*. Dashed lines and grayed out fields indicate hypothesized mechanism in other insects. [Adapted from Tomioka and Matsumoto, 2015 and Pitzschler, 2018. Modified.] ……7

Figure 2: Schematic representation of the putative circadian clock in Antarctic krill – The two main feedback loops are indicated, containing CLK, CYC as positive elements and PER, TIM, and CRY2 as negative elements, whereas negative elemetns interact to suppress the activation of the positive elements. The blue-light photoreceptor CRY1, is activated by light and causes degradation of TIM, releasing PER/TIM suppression from CLK/CYC. Identified clock components in Antarctic krill are colored, while components with no functional characterization are greyed. Modified after Biscontin *et al*., 2017. 10

Figure 3: Study area incl. stations where krill was sampled – A) Krill sampling stations during AMLR 2016 NBP 1606 cruise. B) Stations W011 to W1513 were sampled every 3.5 hours for a time period of 24 h, except for TP06. *E. superba* was caught between 56°- 62°W latitude and 62°- 64°S longitude in the Bransfield Strait between the South Shetlands Islands and the Antarctic Peninsula. UTC-4 = Coordinated Universal Time minus 4 hours, indicates the local time in Bransfield Strait, Antarctica at time of sampling. [Reference: Map Data © 2019 Google. Modified.] 14

Figure 4: Separation of head from the rest of the body of *E. superba* – Head was cut off in a skewed angle behind the eyes without damaging the stomach. The dashed red line indicates the separation. Modified. [Reference: https://link.springer.com/chapter/10.5822/978-1-61091-854-1_1] 17

Figure 5: Schematic representation of circadian oscillators in crustacean head - Localization of the circadian oscillators in the head of a generic crustacean (modified after Strauss and Dircksen, 2010). Putative oscillators are indicated as small sinus waves within the retinae of the compound eye, the eyestalks, and the brain. 17

Figure 6: Separation of *E. superba* head and dissection of tissues – a) Exemplary brain-eyestalks-retinae complex. Dashed red lines indicate the cut surfaces used to separate retinae (R) from eyestalks without contamination and to remove the excess tissues at the base of the brain. b) Exemplary brain-eyestalks complex with dissected retinae. Dashed red lines indicate the cut surfaces used to cut off the eyestalks (ES) from the brain (B). Binocular microscope pictures with a dimensional scaling of 2 mm. 18

Figure 7: Electropherogram (A) and gel (B) of an exemplary eyestalk (left panel) and brain (right panel) sample of Antarctic krill (*E. superba*) - Results of a microfluidic electrophoresis performed in the Agilent 2100 Bioanalyzer using the RNA 6000 Nano Kit System. Time of RNA peak appearance (size related; x-axis) is plotted against the fluorescence (concentration related; y-axis). Small smudgy peaks within the 200 to 1000 nt region usually do indicate degradation, while big bulked peaks within the 2000 to 4000 nt region do indicate genomic contamination. RNA degradation and genomic contamination were not obvious, neither in the electropherogram (A) nor in the progress of the gel (B). The 18S peak resulted from the presence of 18S rRNA which is a component of the small eukaryotic ribosomal subunit, while the 28S peak resulted from the presence of 28S rRNA which is the structural ribosomal RNA for the large subunit of eukaryotic cytoplasmic ribosomes. These two characteristic peaks do suggest that the RNA which was analyzed came from a eukaryotic organism, in this case from the head section of Antarctic krill *E. superba*. 20

Figure 8: Electropherogram (A) and gel (B) of spike 1 (left panel) and 2 (right panel) for *E. superba* samples – Results of a microfluidic electrophoresis performed in the Agilent 2100 Bioanalyzer using the RNA 6000 Nano Kit System. Time of RNA peak appearance (size related; x-axis) is plotted against the fluorescence (concentration related; y-axis). The lower marker of the Kit System showed a peak at 25 [nt], while the spike displayed a peak around 220 [nt]. Both

electropherograms revealed a similar peak pattern (750 nt, 1000 nt, 1800 nt). These peaks could be a result of non-completed DNA digestion, but they do not affect the analyses. For more accurate verification, sequencing would be required. 22

Figure 9: Amplification plots of the TaqManTM Real-Time PCR-Assay – A) Amplification plot of the spike controls 1 and 2 with different concentrations (5 ng, 500 pg, 50 pg, 5 pg, 1.4 pg). B) Amplification plot of the genes *Chryptochrome2* gene (*Cry2*) and *Period* (*Per*). Ct values of *Cry2* reached the threshold baseline (0.1) after approx. 24 cycles, while *Per* Ct values reached the baseline after approx. 26 cycles. The spike concentration (A) which corresponded most likely to this was above 5 pg. For further analyses 7 pg of spike1 and 2 were used. 23

Figure 10: Custom TaqMan^{TM} Array Card format with 13 unique assays and 3 custom controls used in this study – Instead of the mandatory control (CTL) slot 3 custom controls (internal: *Usp46* and external: spike 1 and 2) were loaded. The 8 unique samples were loaded using the ports on the right hand side. Modified. [Reference: https://assets.thermofisher.com/TFS-Assets/LSG/ Warranties/cms_040127.pdf]..... 25

Figure 11: Primer efficiency using clock gene specific primer sets – Mean Ct-values of *Clk* and *Tim* primer sets were plotted against the logarithm of cDNA concentration used in a dilution series (100 ng, 200 ng, 400 ng, and 800 ng) in brain and eyestalks tissue, respectively. Primer efficiencies were calculated using the formula E= ($10^{(-1/slope)}$ -1) x 100. Efficiencies [%] for each primer pair within the respective tissues are indicated in bold. 28

Figure 12: Geometric mean of raw Ct-values of internal and external control - UTC-4 = Coordinated Universal Time minus 4 hours, indicates the local time in Bransfield Strait, Antarctica at time of sampling. Raw mean Ct-values (y-axis) were plotted against the UTC-4 (x-axis). Left panel: Combination of Spike 1 + *Usp46*, respectively in brain. Right panel: Combination of Spike 1 + *Usp46*, respectively in eyestalks. Data are expressed as geometric mean ± SEM (brain: n= 10, 9, 10, 10, 10, 7; eyestalks: n= 10, 10, 10, 10, 10, 7). 30

Figure 13: Heat maps of daily clock gene expression patterns in different tissues – A) Gene expression over time (24 h) in brain. B) Gene expression in eyestalks over time (24 h) (for more details concerning clock gene regulatory network see Figure 1). Heat maps and dendrograms show the expression levels of clock genes during the 24 h cycle and are represented with a color-coded scale; yellow and blue represent high and low expression levels, respectively. TP=

time point, indicates the time point of sampling every 3.5 h in a time period of 24 h (except for TP06, it was 53.5 h). Genes clustered together based on similarity of daily gene expression patterns. Light bar beneath the graphs shows the respective photoperiod at the sea surface (grey = dark phase; yellow = light phase). 33

Figure 14: Core clock gene expression patterns in brain and eyestalks – Ten clock genes (*Clk, Cry2, Cwo, Cyc, Dbt, E75, Per, Sgg, Tim*, and *Vri*) and the metabolic key enzyme *Atpg* were analyzed over 24 h. Relative mRNA levels (NRQ) were plotted against local time (UTC-4). UTC-4 = Coordinated Universal Time minus 4 hours, indicates the local time in Bransfield Strait, Antarctica at time of sampling. Data are expressed as mean ± SEM (brain: n= 10,9,10,10,10,7; eyestalks: n= 10,10,10,10,10,7). TP= time point, indicates the time point of sampling every 3.5 h in a time period of 24 h (except for TP06, it was 53.5 h). Light bar beneath the graph shows the respective photoperiod (grey = dark phase; yellow = light phase) at the sea surface. Schematic sinus curves indicate significant daily oscillation for *Cyc* and *Tim* with a period of 16 h and 24 h in eyestalks determined by RAIN analysis (for *p*-values see appendix) in brain and eyestalks. Hash keys indicate significant differences between both tissues tested for each ZT (Whitney-Wilcoxon test). 37

Figure 15: Associated clock genes and metabolic gene expression patterns in brain and eyestalks – Ten clock genes (*Clk, Cry2, Cwo, Cyc, Dbt, E75, Per, Sgg, Tim*, and *Vri*) and the metabolic key enzyme *Atpg* were analyzed over 24 h. Relative mRNA levels (mean NRQ) were plotted against local time (UTC-4). UTC-4 = Coordinated Universal Time minus 4 hours, indicates the local time in Bransfield Strait, Antarctica at time of sampling. Data are expressed as mean ± SEM (brain: n= 10,9,10,10,10,7; eyestalks: n= 10,10,10,10,10,7). TP= time point, indicates the time point of sampling every 3.5 h in a time period of 24 h (except for TP06, it was 53.5 h). Light bar beneath the graph shows the respective photoperiod (grey = dark phase; yellow = light phase) at the sea surface. Schematic sinus curves indicate significant daily oscillation with a period of 24 h for *Sgg* and *Atpg* in brain and eyestalks, respectively and a daily oscillation with a period of 16 h for *Sgg* in eyestalks. Hash keys indicate significant differences between both tissues tested for each ZT (Whitney-Wilcoxon test). 38

Figure 16: Schematic representation of potential co-regulation of clock genes over idealized 24 h cycle – Mean expression levels of *Clk, Cyc, Per, Tim, Cry2, Cwo, Vri, E75, Sgg, Dbt,* and *Atpg* were analyzed over 18 h +/- 6 hours to identify

putative rhythmicity within a range of periods included between 12 h and 24 h in daily patterns of gene expression. We tested for this range of periods to ensure a detection of all rhythmic circadian behavior, including potential bimodal patterns with 12 h. ‘Hours’ indicates the distance towards the next repetition in hours (potential rhythmicity). TP = time point, displays the time point of sampling every 3.5 h in a time period of 24 h, except for TP06 (it was 53.5 h). Distances between TPs were idealized to 4 hours due to clarity. Blue squares with white ‘B’ illustrate highest NRQ levels in brain, red half round squares with white ‘ES’ illustrate maximum mean expression levels in eyestalks. Half blue/half red squares illustrate maximum expression levels for both tissues at the same time point. Values on y-axis cannot be equated with relative mRNA levels. Genes are grouped in core clock genes (green), associated clock genes (yellow), kinases (purple) and metabolic genes (black). Grey bar indicates dark phase at the sea surface, while yellow field indicates light phase at the sea surface. 46

List of tables

Table 1: Environmental data from August 10th, 11th, and 13th, 2016 – Data were taken in West Antarctica in the Bransfield Strait stratum (62°-64°S, 56°-62°W), between the South Shetland Islands and the Antarctic Peninsula at different stations in August 2016. UTC-4 = Coordinated Universal Time minus 4 hours, indicates the local time in Bransfield Strait, Antarctica at time of sampling. 16

Table 2: Primer sequences of target genes, housekeeping genes, and spike controls used for RT-qPCRs – Sequences of genes were obtained from the krill database (http://krilldb.bio.unipd.it/; Sales *et al.,* 2017) except for spike 1, spike 2 and cry2, which can be accessed via GenBank (https://www.ncbi.nlm.nih.gov/genbank/). 26

Table 3: Primer efficiencies in tested brain tissues – Reaction efficiencies were calculated using the following formula: E = (10(-1/slope) -1) x 100. 53

Table 4: Primer efficiencies in tested eyestalk tissues – Reaction efficiencies were calculated using the following formula: E = (10(-1/slope) -1) x 100. 53

Table 5: Results of statistical RAIN analysis in brain implemented by R - Data were fit to a sinusoidal curve with the required period. *P*-values and the phases of the sinusoidal curve (amplitude of the oscillation is maximal) are shown in the table for each gene. *P*-values were corrected for multiple comparisons using the *false discovery method* (*fdr*) of Benjamini, Hochberg, and Yekutieli (Benjamini and Hochberg, 1995; Benjamini and Yekutieli, 2001) implemented within the RAIN package. Significant *p*-values are indicated in bold. 54

Table 6: Results of statistical RAIN Results of statistical RAIN analysis in brain implemented by R - Data were fit to a sinusoidal curve with the required period. *P*-values and the phases of the sinusoidal curve (amplitude of the oscillation is maximal) are shown in the table for each gene. *P*-values were corrected for multiple comparisons using the *false discovery method* (*fdr*) of Benjamini, Hochberg, and Yekutieli (Benjamini and Hochberg, 1995; Benjamini and Yekutieli, 2001) implemented within the RAIN package. Significant *p*-values are indicated in bold. 54

Table 7: *P*-values of Mann-Whitney-Wilcoxon test - To compare the level of gene expression for each time point (TP) between eyestalk and brain tissues the Mann-Whitney-Wilcoxon test were used. Bold *p*-values were still significant after fdr adjustment. 55

List of abbreviations

Atpg	*Adenosine triphosphate-γ*
B	brain
Clk (CLK)	*Clock* (CLOCK)
Cry2 (CRY2)	*Chryptochrome2* (CHRYPTOCHROME2)
Ct	cycle threshold
CTD	Conductivity, temperature, and depth
Cwo (CWO)	*Clockwork orange* (CLOCKWORK ORANGE)
Cyc (CYC)	*Cycle* (CYCLE)
Dbt (DBT)	*Doubletime* (DOUBLETIME)
DD	dark:dark (24 h darkness)
DVM	diel vertical migration
E	eye
E75	*Ecdysone induced protein 75*
ES	eyestalks
HR3	*nuclear hormone receptor 3*
LD	light: dark (16 h light : 8 h darkness)
NCBI	National Center for Biotechnology Information
NTC	no template control
Per (PER)	*Period* (PERIOD)
RNA	ribonucleic aid
RT	room temperature
-RT	no reverse transcription controls
qPCR	real-time quantitative polymerase chain reaction
Sgg (SGG)	*Shaggy* (SHAGGY)
Tim (TIM)	*Timeless* (TIMELESS)
Usp46 (USP46)	*Ubiquitin specific peptidase 46*
Vri (VRI)	*Vrille* (VRILLE)

1 Introduction

1.1 The Antarctic krill *Euphausia superba*

The Antarctic krill, *Euphausia superba* (Dana, 1850), is an important marine key species of the high-latitudes and belongs to the order Euphausiacea, superorder Eucarida. The term 'krill' originates from the Norwegian word *kril*, describing the small crustaceans North Atlantic whalers found in baleen whales stomachs (Mauchline and Fisher, 1969; Nicol, 1994). Nowadays, the term krill encompasses approx. 85 pelagic shrimp-like crustacean species, also known as Euphausiids, which are widespread in all world oceans (Siegel, 2000). Within the Euphausiids, *Euphausia superba*, our species of interest, dominates the zooplankton communities in the Southern Ocean as an endemic species and is therefore of great importance in the Antarctic marine ecosystem.

E. superba (hereafter krill) is circumpolar distributed in the Southern Ocean between latitudes of approx. 50°S to 70°S (Hill *et al.*, 2013). However, over 70 % of its total population is located in the productive southwest Atlantic sector (Drake Passage) and in the region of the West Antarctic Peninsula, where they inhabit continental shelf areas and slopes as well as deep-ocean basin regions (Siegel, 2000; Atkinson *et al.*, 2004; Siegel, 2016). In the Antarctic food web, krill dominates the herbivorous zooplankton community due to their circumpolar distribution, high abundance, and high biomass (Knox, 1984). This species is of enormous ecological importance since it plays a key role in energy transfer from primary producers (phytoplankton) to higher trophic levels, including fish, squids and top predators such as birds (e.g. penguins, albatrosses, and petrels) and marine mammals (e.g. seals and whales), (Clarke and Harris, 2003).

However, krill's central position in the Antarctic food web might be endangered, to which man contributes directly and indirectly. In course of the anthropogenic climate change, the main feeding grounds of krill in the Southern Ocean, the southwest Atlantic sector and the region of the West Antarctic Peninsula, experienced a surface summer temperature increase of 1°C since the 1950s (Meredith and King, 2005). It is assumed that the decline in sea-ice extent due to warming has led to a change in primary productivity, phytoplankton composition, and sea-ice dynamics (Curran *et al.,* 2003; Clarke and Harris, 2003), and that these changes have already significantly affected the distribution and abundance of Antarctic krill (Atkinson *et al.,* 2004; Reiss *et al*., 2008; Hill *et al.,* 2013). Besides, ocean acidification is also associated with changes in krill population density and

recruitment (Kawaguchi *et al.*, 2013). Furthermore, Atkinson *et al.* (2004) found indications for a decline in krill stocks (~ 70%) over the past 30 years in association with a southward shift of the remaining stocks and an increase in salp densities in the affected regions of the Southern Ocean (Atkinson *et al.,* 2008). Besides the changes in sea-ice extent, the southward shift has also been explained with changes in the anomalies of the Southern Annular Mode (Atkinson *et al.,* 2019).

In addition to the indirect threats of climate change, there is also a direct threat to Antarctic krill stocks in the form of a growing fishing industry (Nicol *et al*., 2012; Reiss *et al*., 2017). The pressure on the species is increased by improved harvesting techniques and a growing interest in newly developed krill products in the aquaculture, pharmaceutical, or dietary supplements sectors due to its high nutritional value (Yoshitomi *et al.,* 2007; Tou *et al.,* 2007; Schiermeier, 2010). In view of the changing environmental conditions within its habitat and increasing commercial interests, a holistic and detailed understanding of Antarctic krill, its adaptability, and its (future) role in the southern polar ecosystem is of great importance.

1.2 Rhythmic functions in the Antarctic krill, *Euphausia superba*

The Southern Ocean is characterized by a wide range of strong seasonal and daily fluctuations, occurring in day length, food supply, and sea-ice extent (Quetin and Ross, 1991; Clarke and Harris, 2003). Antarctic krill show remarkable adaptions to its high-latitude habitat and have evolved rhythmic functions in behavior, metabolism, and transcription to cope with the extreme variations in their environment (Hays, 2003; Murphy *et al.,* 2006; Meyer *et al.,* 2010; Teschke *et al.,* 2011; Piccolin *et al.,* 2018a).

1.2.1 Daily rhythms in krill: diel vertical migration (DVM)

In the water column, adult Antarctic krill usually occur within the upper 200 m in large assemblages or schools with average lengths of hundreds of meters to avoid predation by swarming (Siegel, 2016). A daily rhythm that appears in krill swarms is the diel vertical migration (DVM), (Cisewski *et al*., 2010; Siegel, 2005). The most common DVM pattern, called ‘nocturnal’, describes the zooplankton behavior of swimming upwards towards the surface layers (photic zone) around sunset feeding on phytoplankton, and migrating back downwards towards deeper layers around sunrise (Quetin and Ross, 1991; Hays, 2003). It is generally believed that this strategy has evolved to avoid predator pressure occurring in the light and thus

minimize predator risk (Brierley, 2014). The ‘twilight’ DVM pattern displays another behavior in zooplankton, where two following migrations are performed over a 24 h cycle, one around sunset and another around sunrise (Cohen and Forward, 2005). In an ongoing discussion, light cues are still considered as the main driver of DVM, especially due to the often observed close association between DVM ascent/descent and sunset/sunrise (Cohen and Forward, 2009). Nevertheless, other parameters such as food availability, predator presence/absence (Gliwicz, 1986; Bollens and Frost, 1991; Hays, 2003; Sourisseau *et al.,* 2008) or social interactions (swarming behavior) (Gaten *et al.,* 2008; Kawaguchi *et al.,* 2010) are also taken into account as influencing factors in DVM. Besides, investigations in Arctic zooplankton species showed that DVM patterns correspond with rhythms in metabolic activity and clock gene expression (Häfke *et al*., 2017) and that DVM persists even during winter which suggests the evolvement of an endogenous circadian clock mechanism (Last *et al*., 2016).

It has been suggested that Antarctic krill can flexibly adapt their DVM pattern to environmental factors such as predator or food conditions (Zhou and Dorland, 2004; Cisewski *et al*., 2010). Moreover, as a high latitude species, it might be possible that krill DVM patterns vary between seasons (Piccolin *et al*., in prep). In spring and autumn the ‘nocturnal’ DVM in krill is more pronounced due to a clear day/night cycle and ranges between 50 and 150 m depth, compared to summer where krill DVM is restricted within surface layers possibly due to high food availability and weaker photoperiodic cues (Siegel, 2005; Quetin and Ross, 1991). In winter, krill may become more benthopelagic living in deeper layers around 350 to 600 m and might perform extensive DVM, remaining below 100 m during the night, and sinking down to around 300 m during daytime (Siegel, 2005). The influence of photoperiodic cues and endogenous rhythms on krill DVM was investigated by Gaten *et al.* (2008), where different rates of activity were detected under constant light/dark conditions. Therefore, they assumed that the photoperiod might not be the major factor in regulating krill DVM, but rather that an endogenous timing system which is instead influenced by an interplay of local food conditions, social interactions, and the light-dark cycle might be involved. Daily rhythms in krill oxygen consumption and energy metabolism which were higher in the laboratory during the dark phase might represent a connection between nocturnal krill DVM patterns and daily rhythms of metabolic regulation (Teschke *et al.,* 2011).

1.2.2 Seasonal cycles in krill

The high-latitude habitat of krill in the Southern Ocean displays strong seasonal variabilities affecting the dynamics of abiotic and biotic factors over the year. In summer, the environment displays day length of up to 24 h combined with a lack of sea-ice cover, leading to high levels of irradiance at sea surface and increasing primary production. In winter, the situation differs, showing shortened day length (3-4 h light) and extreme sea-ice extent which leads to a significantly reduced irradiance at sea surface and to the absence of primary production.

To cope with these extreme high-latitude challenges, krill display seasonal cycles of metabolic activity, sexual maturity, and lipid utilization. Adjustments such as low metabolic rates (Teschke *et al.,* 2011; Meyer, 2012; Piccolin *et al.,* 2018b) sexual regression (Kawaguchi *et al.,* 2007) and high lipid utilization (Meyer *et al.,* 2010) are observed in winter, whereas high metabolic rates (Teschke *et al.,* 2007), sexual maturity (Kawaguchi *et al.,* 2006), and low lipid utilization (Teschke *et al.,* 2008) are common during summer. These sequences of seasonal cycles of energy utilization and energy storage should benefit krill during low-food seasons and contribute to an over-wintering strategy (Meyer, 2012). Food availability is generally supposed to be a major driving force behind krill maturity and metabolism as they often correlate in the field, but it is also suggested that metabolic activities might be driven by another different regulatory mechanism (Torres *et al.,* 1994).

On the basis of several laboratory studies, it was concluded that the actual driving mechanism could be the prevailing photoperiod. Indeed, the reaction of krill to high food supply during artificial winter light conditions depended on the prevailing light regime and feeding activity increased with prolonged light period (Atkinson *et al*, 2002; Teschke *et al.,* 2007; Meyer *et al.,* 2010). In different studies, both sexual maturity and sexual regression in krill were also influenced by changes in artificial seasonal light periods (Teschke *et al.,* 2008; Brown *et al.,* 2010). In fact, under constant dark conditions in the laboratory over months or even years, seasonal changes in krill sexual maturity and metabolic activity were observed (Brown *et al.,* 2013, Kawaguchi *et al.,* 2007, Piccolin *et al.,* 2018b). In one of the latest studies, Piccolin *et al.* (2018b) ascertained that the annual light regime could possibly trigger the seasonal cycle of metabolic activity in Antarctic krill. In long-term laboratory experiments they simulated seasonal light regimes and detected photoperiodic effects on krill's metabolic cycle which were also found on gene expression levels (Seear *et al.,* 2009). Ultimately, this leads to the assumption that the seasonal

cycles in krill are regulated by an endogenous timing system synchronized to the seasonal light conditions in the Antarctic.

1.3 Daily biological processes in organisms are regulated by endogenous clocks

Life on land and in the oceans is determined by multiple rhythmic events, the best known being probably the day/night cycle, the tides, and the annual change of seasons. Because of these rhythmic changes, most organisms have synchronized their physiology and behavior to their environment and therefore evolved an endogenous timing system often referred to as endogenous biological clock (Dunlap, 1999; Strauss and Dircksen, 2010). An endogenous clock system represents a molecular oscillator that is synchronized by rhythmic environmental cues (*Zeitgeber*, German = time giver) and can respond to them through rhythmic output functions at the metabolic, physiological, or behavioral level. Ultimately, the three classic features of a biological clock are an entrainment to relevant environmental cues, a free-running period, and temperature compensation (Kuhlman *et al.,* 2007; Zhang *et al.,* 2013). Hence, biological clocks have the ability to maintain constant endogenous rhythmicity over a wide temperature range and in the absence of environmental time cues.

1.3.1 The circadian clock regulating biological processes

The circadian clock (from the Latin ‘circa dies’ = ‘about a day’) is the most studied endogenous timing system in all groups of organisms, including plants, animals, fungi, or photosynthesizing cyanobacteria. It is basically a series of circadian or endogenous rhythms that oscillate under constant conditions within 24 h and persist even in the absence of entraining environmental cues (Bell-Pedersen *et al*., 2005; Kuhlman *et al.*, 2007). In this case, an internal pacemaker, or clock, controls the endogenous rhythmicity and provides autonomous control of cellular activity levels, thus regulating physiology, metabolism, and behavior in an oscillatory pattern (Strauss and Dircksen, 2010). The most reliable cue affecting the synchronization of the clock and therefore regulating daily rhythms is represented by the day/night cycle, thus light can be considered as the main ‘*Zeitgeber’* for the circadian clock. Other kind of cues including food availability, temperature, and social behavior are also considered as additional *Zeitgebers* (Gaten *et al.*, 2008; Bell-Pedersen *et al*., 2005; Kronfeld-Schor *et al.,* 2017).

1.3.2 The circadian clock on a molecular level using the example of *Drosophila*

At the molecular level, the circadian clock is based on rhythmically expressed so called 'clock genes', which are so diverse and interact in such different ways that an independent evolution of the circadian clock in all organisms can be assumed (Dunlap, 1999). The best-studied model organism in terms of eukaryotic circadian clock systems is the fruit fly *Drosophila melanogaster* and is therefore used as an example in the following.

Central to the circadian clock of *Drosophila* are negative and positive transcriptional and translational feedback loops controlled by a set of clock genes (Dunlap, 1999). Transcriptional feedback loops consist of sequence-specific DNA binding proteins which stimulate the transcription of their own repressors, thus causing a negative feedback loop (Hardin, 2009). At the beginning, the core clock genes *Clock* (*Clk*) and *Cycle* (*Cyc*) interact by forming the CLK/CYC heterodimer, and activating respective gene expression by binding to E-box sequences in target promoters (Fig. 1) (Tomioka and Matsumoto, 2015). Within the first feedback loop, the heterodimer CLK/CYC activates the transcription of the core clock genes *Period* (*Per*) and *Timeless* (*Tim*) around sunset. In a self-sustained negative feedback loop, the transcribed proteins PER and TIM accumulate in the cytoplasm forming the heterodimer PER/TIM at midnight, and translocate into the nucleus to suppress their own transcription by inhibiting the DNA-binding ability of CLK/CYC. The timing of the nuclear entry is regulated through phosphorylation of PER and TIM by the protein kinases SHAGGY (SGG) and DOUBLETIME (DBT). Following this, mRNA levels of *Per* and *Tim* decrease to a minimum around dawn and a new cycle of transcriptional activation is then started during the early day.

Furthermore, two additional feedback loops with the associated clock genes *Vrille* (*Vri*) and *Clockwork orange* (*Cwo*) were identified in *Drosophila* involving the CLK/CYC heterodimer. Hence, CLK/CYC activates the transcription of the repressor *Vri* and *Par domain protein 1ε* (*Pdp1ε*), whereby VRI proteins accumulate suppressing the transcription of *Clk* through a V/P box in the *Clk* regulatory region. As PDP1ε is accumulating later than VRI, there is a period of time for *Clk* transcription and accumulation of CLK during the day. The mechanism underlying cyclic expression of *Cyc* gene remains to be understood. In other insects, this regulatory function is assumed to be fulfilled by *nuclear hormone receptor 3* (*HR3*) and *ecdysone induced protein 75* (*E75*) that are also involved in regulation of molting (Tomioka and Matsumoto, 2015). The general function of this process is still not clear. In the second additional feedback loop, CLK/CYC activates the

transcription of the repressor *Cwo* suppressing CLK/CYC-mediated transcription and thus regulates the amplitude of *Per* and *Tim* mRNA oscillation. A loss of *Cwo* results in altered molecular and behavioral rhythms, suggesting this feedback loop might promote robust rhythmicity.

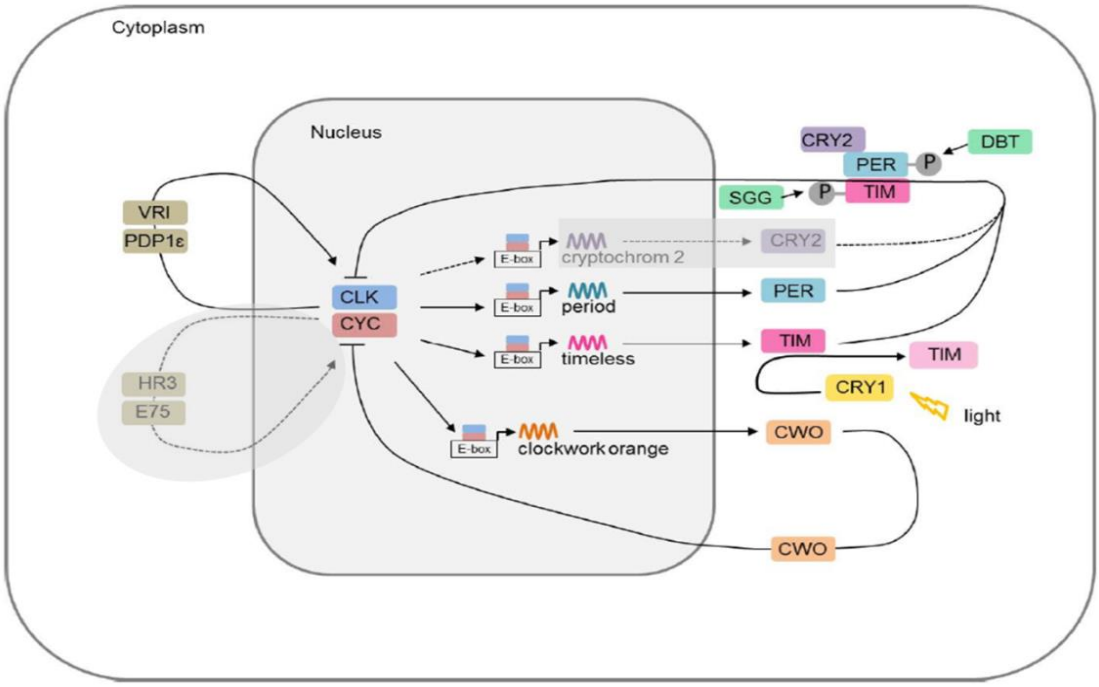

Figure 1: Hypothetical molecular mechnisms of the insect circadian clock in the model organism *Drosophila melanogaster* – The principal auto regulative feedback loop consists of the transcription factors CLOCK (CLK) and CYCLE (CYC), and the regulators PERIOD (PER) and TIMELESS (TIM). In *Drosophila,* CHRYPTOCHROME (CRY1) displays a negative regulator and degrades TIM in a light-dependent manner to reset the clock's phase. CHRYPTOCHROME (CRY2) as an additional negative regulator is not present in Drosophila, but in other arthropods species including the monarch butterfly *Danaus plexippus* (Zhu *et al*., 2008; Merlin *et al*., 2009) and the Antarctic krill (Biscontin *et al*., 2017). SHAGGY (SGG) and DOUBLETIME (DBT) regulate the timing of nuclear entry of TIM and PER by phosphorylating both proteins, respectively. In an additional loop, CLK is cyclically expressed by VRILLE (VRI) and PAR DOMAIN PROTEIN 1ε (PAR1ε), while expression of CYC is still unknown in *Drosophila*, but proposed to be expressed by HR3 and E75 in other insects. In a second additional loop, CLOCKWORK ORANGE (CWO) is rhythmically expressed. Solid lines indicate pathways known for *Drosophila*. Dashed lines and grayed out fields indicate hypothesized mechanism in other insects. [Adapted from Tomioka and Matsumoto, 2015 and Pitzschler, 2018. Modified.]

Most circadian clock processes on a molecular level happen in a similar way also in organisms such as mammals or other insects. However, the circadian clock of *Drosophila* differs by the presence of the clock gene *Cryptochrome* (*d-Cry* or *Cry1*), a blue light photoreceptor, which promotes the light-dependent degradation of TIM, hence entraining the endogenous clock system (Tomioka and Matsumoto, 2015). In addition to *Cry1*, the clock gene *cryptochrome2* (*m-Cry* or *Cry2*) is present in

mammals and other arthropods (Rubin *et al.,* 2006; Merlin *et al.,* 2009), where the mRNA expression level peaks at sunset (as levels of *Tim* and *Per*) and the transcribed protein CRY2 forms a complex with PER/TIM to inhibit CLK/CYC. In contrast to CRY1, CRY2 has lost the ability of photoreception (Tomioka and Matsumoto, 2015).

1.3.3 The circadian clock in marine organisms

In terrestrial animals, circadian clocks are well-studied using model organisms in arthropods or mammals (such as *Drosophila* and mouse). Far fewer studies have investigated the principles of the circadian clock in marine organisms. Terrestrial and marine organisms are exposed to different rhythmic environmental cues (e.g. tidal rhythm) due to their physical habitat, which may lead to different timekeeping functions (Tessmar-Raible *et al.,* 2011). In the marine environment, some studies revealed an effect of temperature (Lahiri *et al.,* 2005) and food availability (Cavallari *et al.*, 2011; Aguzzi *et al.,* 2011) on circadian clocks and furthermore assume an influence on circadian clock functions by endogenous noncircadian clocks (Zantke *et al.,* 2013). Rhythmic circadian behaviors can include rhythms of feeding/fasting, rhythms of sleep/wake or rhythms related to reproduction (e.g. mating and spawning) and are not restricted to periods of 24 h including also bimodal patterns with 12 h periods (e.g. to cope with tidal cycles) (Tessmar-Raible *et al.,* 2011; Gaten *et al*., 2008).

Among others, circadian rhythmicity activities incl. clock functions have also been investigated in crustaceans, for example in relation to locomotion, reproduction, metabolism, and developmental processes (Strauss and Dircksen 2010). The pacemaker of circadian clocks in crustacea, as in many other animals, is located in the nervous system. For the intertidal isopod *Eurydice pulchra* tidal cycles of swimming in parallel to circadian 24 h rhythms in behavioral, physiological, and molecular phenotypes were demonstrated by Zhang *et al.* (2013), with the assumption that the circadian pacemakers are located in the brain. In the Norwegian lobster *Nephrops norvegicus*, candidate clock genes including a vertebrate-like *Cry2* were identified within the eyestalk tissues of the species (Sbragaglia *et al.,* 2015). So far, no crustacean single central brain oscillator or master has been identified (Strauss and Dircksen 2010). Therefore, Strauss and Dircksen (2010) assumed that several neuronal tissues might act together in a complex system, which contains distinct oscillators located in the brain (supraoesophageal ganglion), the retina of the eye, the eyestalks, and the caudal photoreceptors.

1.4 The circadian clock in *Euphausia superba*, and mechanisms of regulation

The level of knowledge of circadian regulation in non-model marine organisms is low, and even less is known about those regulations in high-latitude pelagic zooplankton species like the Antarctic krill. As a pelagic species, krill might not be affected by tidal rhythms but they still perform DVM and are therefore subjected to daily changes in light spectral composition and light intensity.

As one of the first, Mazzotta *et al*. (2010) recorded circadian clock gene activity over 24 h in wild krill during Antarctic summer and identified the presence of *Cryptochrome2* (Es*Cry2*), a krill orthologue of the mammalian-like *Cry2* (*m-Cry2*) gene. Although an ancestral form of circadian feedback loop was assumed in krill because of the presence of Es*Cry2*, daily expression levels did not coincide with previous findings in the honeybee, *Apis mellifera*, and in the monarch butterfly, *Dana plexippus* (Rubin *et al*., 2006; Zhu *et al*., 2008). However, entrainment of clock functions may follow the rhythms of alternative *Zeitgebers*, since even in the absence of clear light/dark cues daily *Cry2* expression levels showed daily oscillation. Mazzotta *et al*. (2010) supposed light spectral composition to be the major influence, since Es*Cry2* oscillation did not show any apparent link with the daily cycle of light intensity. Based on these field findings, Teschke *et al*. (2011) conducted laboratory analyses to determine if an endogenous rhythm could be detected in krill clock gene activity at the molecular level and whether the regulation of rhythmic output functions in physiology was influenced. During the experiments, daily gene expression of Es*Cry2* were determined under simulated long-day conditions (16 h light: 8 h darkness, LD 16:8) and constant darkness (DD). Under both conditions *Cry2* displayed daily oscillation in mRNA levels, which also correlated with metabolic-related enzyme activity profiles underlying the endogenous nature of the circadian timing system in krill with a putative link to metabolic key processes (Teschke *et al*., 2011). Summer field samples of Mazzotta *et al*. (2010) were used in the laboratory analysis of De Pittà *et al*. (2013) investigating the krill transcriptome over daily cycles. Daily oscillations with periods of either 24 h or 12 h were detected for 8 % of the transcriptome reflecting a chronological progression of biochemical and physiological events throughout the 24 h cycle. Thus an endogenous circadian clock seems to control the krill metabolism in the high-latitude environment during summer.

The most important findings for the functional characterization of the circadian clock in krill came from Biscontin *et al.* (2017) and Hunt *et al*. (2017), who identified putative krill orthologues of the core clock components by screening online

databases containing the krill transcriptome (Hunt *et al*., 2017; Sales *et al*., 2017). Beyond that, Biscontin *et al*. (2017) proposed a circadian clock model for the Antarctic krill and defined the role of core clock components within the circadian feedback loop (Fig. 2). Within the core feedback loop, the krill clock proteins CLK (EsCLK) and CYC (EsCYC) displayed the positive regulators, like in *Drosophila*, whereas PER (EsPER), TIM (EsTIM), and CRY2 (EsCRY2) displayed putative negative regulators, like in the monarch butterfly, *D. plexippus*. In krill, EsPER and EsTIM interacted with various kinases among others EsSGG, EsDBT, or EsVRI. Significant daily rhythmic expression patterns in krill were observed for the core clock genes *EsClock*, *EsCycle*, *EsPeriod*, *EsTimeless*, and *EsCryptochrome2* (Biscontin *et al*., 2017). Despite the strong annual variability at high-latitude regions, light is still suggested as main *Zeitgeber* in krill with a light-entrainment occurring among others through the blue-light photoreceptor CRY1 (EsCRY) and krill opsins (Biscontin *et al*., 2016; Biscontin *et al*., 2017; Piccolin *et al*., 2018b).

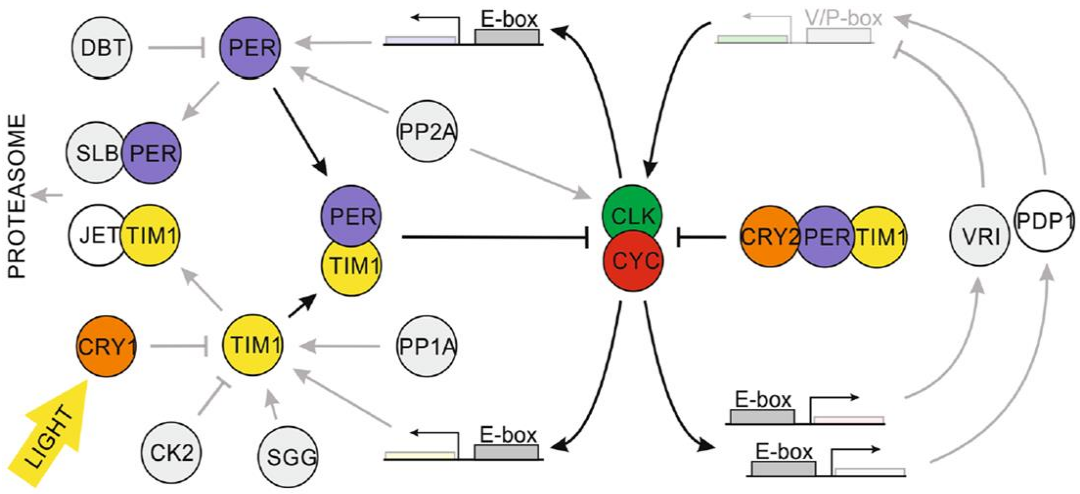

Figure 2: Schematic representation of the putative circadian clock in Antarctic krill – The two main feedback loops are indicated, containing CLK, CYC as positive elements and PER, TIM, and CRY2 as negative elements, whereas negative elemetns interact to suppress the activation of the positive elements. The blue-light photoreceptor CRY1, is activated by light and causes degradation of TIM, releasing PER/TIM suppression from CLK/CYC. Identified clock components in Antarctic krill are colored, while components with no functional characterization are greyed. Modified after Biscontin *et al*., 2017.

1.5 Challenges to circadian regulation in high-latitude species

The control of biochemical and physiological processes by an endogenous circadian clock plays a central role in the adaptive success of the high-latitude key species Antarctic krill, especially in the regulation of DVM and the seasonal life cycles. One persisting question is if the circadian regulation incl. clock functions remains active during summer and winter due to the extreme kight conditions at those times of the year. Circadian timing mechanisms and potential regulation were studied both in wild krill during summer conditions (Mazzotta *et al*., 2010; de Pittà *et al*., 2013) and in the laboratory under different artificial seasonal light regimes (Piccolin *et al*., 2018; Teschke *et al*., 2011; Biscontin *et al*., 2017), but still information on clock gene activity and rhythmic activities promoted by alternative light cues is scarce. In addition, according to our knowledge, field studies concerning the circadian clock functions in krill during winter conditions are still missing. Moreover, the current increasing anthropogenic-driven warming accelerates changes in the Southern Ocean environment, which might affect the synchronization between endogenous and external factors, creating a 'match-mismatch' scenario in circadian rhythmicity with potential negative effects for the occurring krill population. Hence, it is essential to investigate the capability of krill to regulate their endogenous circadian timing system under natural extreme environmental changes during seasons.

1.6 Aim of study

The present study investigated clock gene expression in wild Antarctic krill during winter conditions to give a first basic impression about what happens in clock functions, since so far only field studies in summer have been conducted. Within this thesis, wild krill from the Bransfield Strait, Southern Ocean, were sampled every 3.5 h over a 24 h cycle during a winter cruise in order to examine:

i) putative rhythmic gene expression patterns of clock genes (*Clock*, *Cycle*, *Period*, *Timeless*, *Cryptochrome2*, *Doubletime*, *Shaggy*, *Clockwork orange*, *Vrille*, *E75*) and the metabolic gene *Atpg*.

Additionally, previous findings regarding clock gene expression in krill under laboratory and field conditions often showed high variance among biological replicates together with low amplitude of different gene expression, leading to poor statistical power to detect significant rhythmicity. In order to optimize these sources of interference, a tissue-specific examination was tested in the present work with the following sub-targets:

ii) tissue-specificity of clock gene expression in different tissues (brain and eyestalks) to identify potential interactions or co-regulations between clock genes and specific tissues

iii) efficiency of different clock gene primer sets (*Clock* and *Timeless*) to draw conclusions on the accuracy of clock gene expression quantification in different tissues of krill

2 Material & Methods

2.1. Time-series sampling of *E. superba* in the field

Field samples of *E. superba* from a 24 h time series were collected in austral winter in the Atlantic sector of the Southern Ocean. The RNA of brain and eyestalks tissues was extracted and converted to cDNA. Via TaqMan™ qPCR and a modified $2^{-\Delta\Delta Ct}$ normalization method, daily gene expression profiles of clock genes were generated and tested for rhythmicity (between 12h and 24 h) or significant differences among tissues.

Samples of *E. superba* were collected in West Antarctica in the Bransfield Strait (62°-64°S, 56°-62°W), between the South Shetland Islands and the Antarctic Peninsula. Different stations were sampled between 4th and 31st August 2016 in the framework of the Antarctic Marine Living Resources (AMLR) program, during the voyage NBP1606 with the research icebreaker RVIB *Nathaniel B. Palmer* from the National Oceanic and Atmospheric Administration (NOAA). Krill were caught using a 1.8 m (2.54 m² mouth area) Isaacs-Kidd midwater trawl (IKMT) equipped with a 505 µm mesh net. The volume of sea water filtered during trawlings, was quantified using a General Oceanic flow meter (model 2930R) attached on the depressor frame in front of the net. All tows were double-oblique to 170 meters (m) depth of the water column. Real-time tow depths were deduced from a pressure sensor mounted on the trawl bridle. Tow speeds were ~2 knots, with volumes filtered averaging ~3621 m³. Krill abundance was standardized to no. m^{-2} based on volume of water filtered at each time point multiplied by the depth of the tow. To get a time series covering one entire 24 h cycle, *E. superba* was caught with a regular time interval of 3.5 hours within Bransfield Strait starting on 22:00 on August 10th until 12:00 on August 11th for a total of 5 time points (TP). The last time point (TP06) of the time series was collected at 17:30 on 13th August (Fig. 3, Tab. 1). The longer interval of time occurring between TP05 and TP06 was due to unfavorable weather conditions together with operational issues regarding the sampling grid schedule of the AMLR expedition. The biomass of adult *E. superba* between time points and stations were highly variable, ranging from 0.57 no. m^{-2} on August 10th (22:00 UTC-4) over 651 no. m^{-2} (01:30 UTC-4), 13 no. m^{-2} (08:30 UTC-4), and 1064 no. m^{-2} (12:00 UTC-4) on August 11th to 21.4 no. m^{-2} on August 13th (Tab. 1).

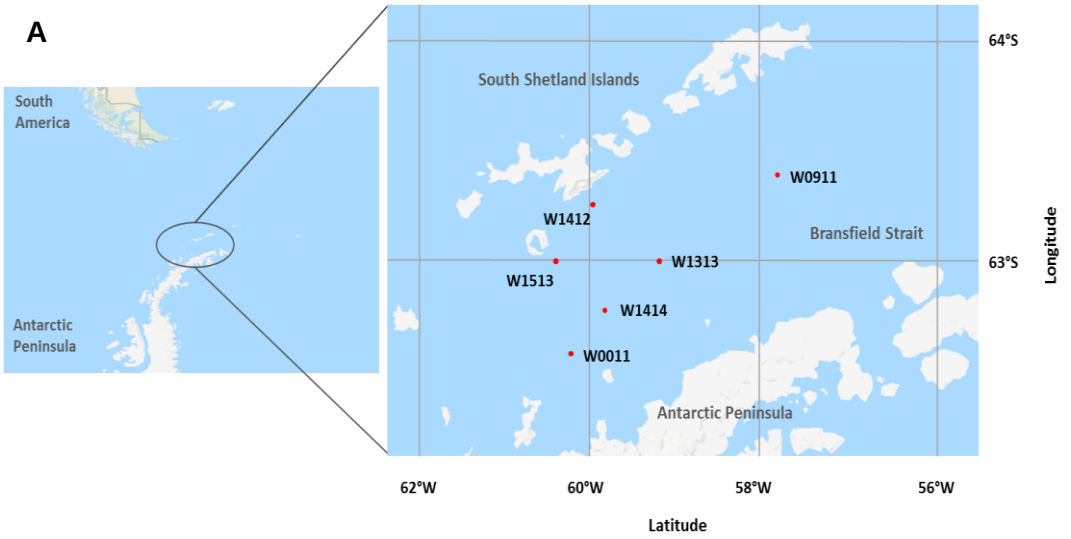

B

Date	Station	Station coordinates	Sampling time point (UTC-4)	Time point
08/10/2016	W0011	63°28'S, 60°26'W	22:00	TP01
08/11/2016	W1414	63°15'S, 60°0'W	01:30	TP02
08/11/2016	W1513	63°0'S, 60°25'W	05:00	TP03
08/11/2016	W1412	62°45'S, 60°0'W	08:30	TP04
08/11/2016	W1313	63°0'S, 59°30'W	12:00	TP05
08/13/2016	W0911	62°29'S, 57°31'W	17:30	TP06

Figure 3: Study area incl. stations where krill was sampled – **A)** Krill sampling stations during AMLR 2016 NBP 1606 cruise. **B)** Stations W011 to W1513 were sampled every 3.5 hours for a time period of 24 h, except for TP06. *E. superba* was caught between 56°- 62°W latitude and 62°- 64°S longitude in the Bransfield Strait between the South Shetlands Islands and the Antarctic Peninsula. UTC-4 = Coordinated Universal Time minus 4 hours, indicates the local time in Bransfield Strait, Antarctica at time of sampling. [Reference: Map Data © 2019 Google. Modified.]

2.2 Average integrated chlorophyll *a* determination and water temperatures

Chlorophyll *a* (chl *a*) concentration is used as a proxy for the available food in the water column for Antarctic krill. At each station, conductivity, temperature, and depth (CTD) were measured with a SBE9/11 (SBE Inc.), equipped with 10 l bottles for water sampling. These bottles were closed during the upcast at 750, 200, 100, 75, 50, 40, 30, 20, 15, and 5 m respectively. Chlorophyll *a* concentrations were detected fluorometrically following Holm-Hansen *et al*. (1965) and for each station the average integrated chl *a* (to 100 m depth; mg chl *a* m^{-2}) was calculated (Reiss *et al.,* 2009). The average chl *a* concentration was generally higher during daytime with values of 6.38 and 7.28 mg chl *a* m^{-2} (August 11th, 12:00 and August 13th, 17:30) compared to nighttime where measured chl *a* concentrations varied between ~ 3.5

to 5.0 (August 11th 01:30 to 08:30) (Tab. 1). There are no chl *a* and temperatures data for August 10th. The water temperatures remained constant between -1.80°C during the day and -1.30°C during the night (Tab. 1).

2.3 Irradiance at fishing depth and sea-ice concentration data

Surface irradiance was measured with the Biospherical Instruments' Quantum Scalar Reference Sensor (QSR-240) on mast the research vessel. The QSR-240 is a surface (non-submersible) instrument for monitoring total incident photosynthetically active radiation from the sun and sky. Photosynthetically available radiation (PAR) denotes the spectral range of solar radiation from 400 to 700 nanometers utilized by photosynthetic organism to perform photosynthesis. Measured PAR at surface in the Bransfield Strait was indicated in units of µEinstein/m²/s² and was converted to W/m² to determine irradiance at sampling depth (1 W/m² ≈ 4.6 µEinstein/m²/s²). The actual solar irradiance at 170 m depth was calculated according to Mazzotta *et al*., (2010) using the following formula:

$$I_Z = I_0 e^{-(K_d Z)}$$

For all time points, the calculated irradiance at fishing depth was very low (Tab. 1). At the surface, we found a light/dark cycle with sunrise approx. at 08:00, sunset approx. at 16:00 and dusk at approx. 17:00 UTC-4 and irradiance at the sea surface of 2 to 8 W/m² during the day and of 34 W/m² at dusk. However, we must consider that: i) at fishing depth, the actual levels of irradiance might have been extremely low over the entire 24 h cycle (Tab. 1) and ii) due to DVM and/or twilight DVM before sampling, *E. superba* might have occurred at different depths with respect to the actual fishing depth. Therefore, it is impossible to predict the exact photoperiod to which krill was exposed, but we can assume that krill were exposed to a maximum of 8 daily hours of light (when occurring close to the surface at all times) and a minimum of almost zero daily hours of light (when occurring at fishing depth or deeper at all times).

Sea-ice concentration data for August 10th, 11th and 13th, 2016 were extracted from the U.S. National Ice Center (https://www.natice.noaa.gov). The ice concentration is reported in tenths (0/10 to 10/10). For August 10th and 11th, the sea-ice concentration showed consistent low values of 1-3 tenths with new and young ice, while on August 13th the ice concentration rose slightly to 4-6 tenths (Tab. 1).

Table 1: Environmental data from August 10th, 11th, and 13th, 2016 – Data were taken in West Antarctica in the Bransfield Strait stratum (62°-64°S, 56°-62°W), between the South Shetland Islands and the Antarctic Peninsula at different stations in August 2016. UTC-4 = Coordinated Universal Time minus 4 hours, indicates the local time in Bransfield Strait, Antarctica at time of sampling.

Date	Station	Sampling time point (UTC-4)	Time point	Light conditions during sampling	Irradiance at fishing depth (W/m^2)	*E. superba* adult abundance (no. per 1000 m^2)	Average chl *a* (mg per m^2)	Average temperature (°C)	Sea ice concentration (tenths)
08/10/2016	W0011	22:00	TP01	☾	0,000000084	0.57	NA	NA	1-3
08/11/2016	W1414	01:30	TP02	☾	0,000000084	651.31	4.18	-1.88	1-3
08/11/2016	W1513	05:00	TP03	☾	0,000000084	589.08	3.48	-1.27	1-3
08/11/2016	W1412	08:30	TP04	☾ / ☼	0,000000084	13.23	5.03	-1.30	1-3
08/11/2016	W1313	12:00	TP05	☼	0,000000336	1064.16	6.38	-1.79	1-3
08/13/2016	W0911	17:30	TP06	☼ / ☾	0,000001408	21.40	7.28	-1.85	4-6

average chl *a: in the upper 100 m

***average temperature**: in the upper mixed layer (200 to 300 m depth)

***irradiance**: calculated as in Mazzotta *et al*.,2010

2.4 Selecting and processing of *E. superba*

Immediately after each IKMT trawl, all zooplankton were sorted and krill was separated first. Hence, a subsample of up to 100 adult krill was measured. Total body length (mm) was determined by measuring the distance from the tip of the rostrum (forward extension of the carapace) to the posterior tip of the uropods (appendages of the last body segment) (Standard 1 as described by Mauchline, 1980). After measuring, krill was directly frozen in liquid nitrogen and stored at -80°C until further processing.

From each subsample, we selected the experimental krill to use for molecular analysis based on the following parameters: (i) body lengths between 40 and 50 mm to ensure same development stages and a sufficient amount of RNA; (ii) a balanced male/female ratio; (iii) damaged samples were neglected. Based on these parameters, it was possible to select 10 biological replicates per time point, with the exception of TP06 where only 7 samples were suitable for further chronobiologic analyses. In total, 57 frozen *E. superba* sampled during AMLR2016 cruise were chosen for brain- and eyestalk-specific gene expression analysis.

2.4.1 Tissue separation and processing

In a first step, the head was separated from the rest of the body. Therefore each frozen krill sample was stored on dry ice and the head was cut off with a scalpel in a skewed angle directly behind the eyes without damaging the stomach (Fig. 4). Heads were stored in pre-chilled 1 ml RNA*later*™-ICE Tissue Transition Solution

(Thermo Fisher Scientific, Invitrogen™ Ambion Life technologies, USA) overnight (at least 16 h) at -20°C in 2 ml Eppendorf™ Safe-Lock Tubes (Eppendorf AG, Germany) to allow thawing with minimized RNA degradation. After cleaning heads from antennae, endopods, and chitin the remaining brain-eyestalks-retinae complexes (Fig. 5a) were retransferred into the 1 ml RNA*later*™-ICE solution and kept at -20°C for later dissections of tissues.

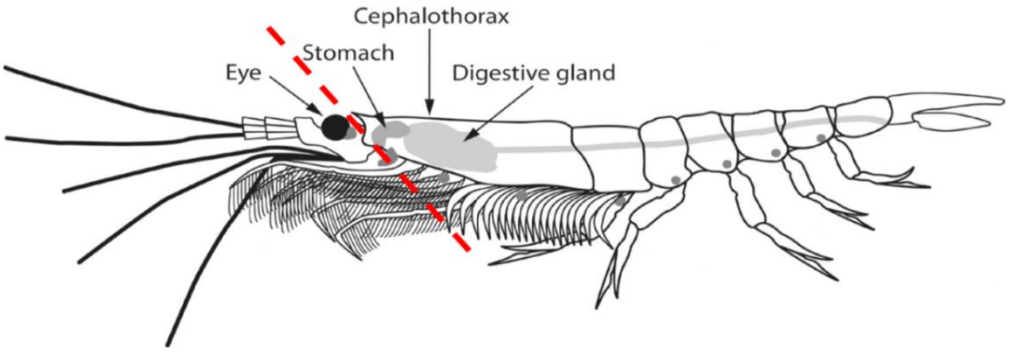

Figure 4: Separation of head from the rest of the body of *E. superba* – Head was cut off in a skewed angle behind the eyes without damaging the stomach. The dashed red line indicates the separation. Modified. [Reference: https://link.springer.com/chapter/10.5822/978-1-61091-854-1_1]

2.4.2 Dissection of eyestalk and brain tissue

Putative circadian oscillators are assumed to be found in the head of crustacean in particular within the retinae of the compound eye, the eyestalks, and the brain (Strauss and Dircksen 2010; Fig. 5). Based on this assumption, we decided to measure clock gene expression in the eyestalks and in the brain of *E. superba*. We excluded the retinae because clean RNA extraction was not possible due to contaminations by visual pigments.

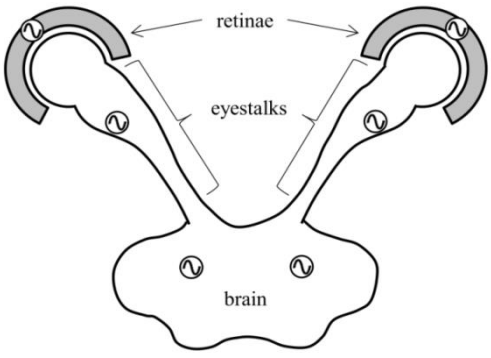

Figure 5: Schematic representation of circadian oscillators in crustacean head - Localization of the circadian oscillators in the head of a generic crustacean (modified after Strauss and Dircksen, 2010). Putative oscillators are indicated as small sinus waves within the retinae of the compound eye, the eyestalks, and the brain.

Dissection of eyestalk and brain tissues was performed under a binocular microscope (Leica MZ125) with cooling chambers for Petri dishes keeping the samples chilled (~2°C). The brain-eyestalks-retinae complexes (Fig. 6a,b) were dissected into brain (B), eyestalks (ES), and retinae (R) by using tweezers and fine scissors. First, the retinae were separated from the eyestalks. It was cut as close as possible to the transition zone between retinae and eyestalks (see rounded dashed line near retinae, Fig. 6a), avoiding contaminations of the eyestalks by visual pigments from the retinae. Any remnants of pigments on the eyestalks were carefully removed prior to RNA extraction to avoid possible interferences during RNA concentration measurements. Hereafter, eyestalks (ES) were severed near the brain (B) (Fig. 6b) and chitin leftovers as well as irrelevant tissues were removed from the brains (see straight dashed line Fig. 6a). The separated retinae of the krill samples were stored in 500 µl RNA*later*™-ICE Tissue Transition Solution and were not further used for this study. Dissected brain and eyestalk tissues were stored individually in 300 µl RNA*later*™-ICE solution at -20°C for later RNA extraction.

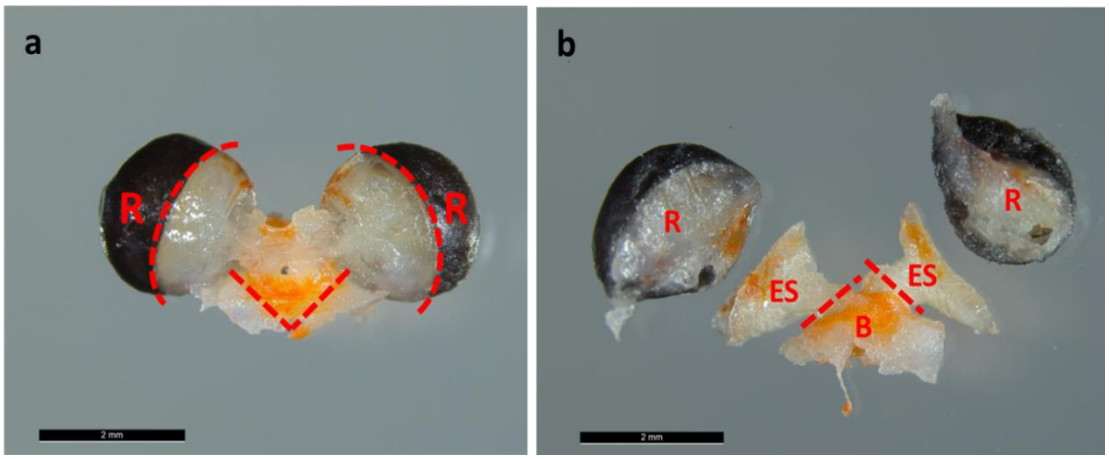

Figure 6: Separation of *E. superba* head and dissection of tissues – **a)** Exemplary brain-eyestalks-retinae complex. Dashed red lines indicate the cut surfaces used to separate retinae (R) from eyestalks without contamination and to remove the excess tissues at the base of the brain. **b)** Exemplary brain-eyestalks complex with dissected retinae. Dashed red lines indicate the cut surfaces used to cut off the eyestalks (ES) from the brain (B). Binocular microscope pictures with a dimensional scaling of 2 mm.

2.5 RNA extraction

RNA of eyestalks and brain tissues was extracted using the Direct-zol™ RNA MicroPrep kit (Zymo Research, USA). Before tissue homogenization, 300 µl chilled TRIzol™ Reagent (Thermo Fisher Scientific, USA) was pipetted into 0.5 ml Precellys™ tubes (Bertin Technologies S.A.S, France) containing 1.4 mm ceramic

(zirconium oxide) beads. The tissues stored in RNA*later*™-ICE were dried on KimWipes™ tissues (Kimberly-Clark Professional™ Corporation, USA), weighed, and transferred into the prepared Precellys™ tubes. The subsequent homogenization was performed by using the Precellys™ 24 homogenizer (Bertin Technologies S.A.S, France) for 2x15 seconds (s) at 5000 rounds per minute (rpm) and 4°C. Homogenates were incubated at room temperature (RT, 20-25°C) for 5 minutes (min). For phase separation, 60 µl chloroform (Sigma-Aldrich, USA) was added to the Precellys™ tubes and tubes were thoroughly inverted and vortexed. After an incubation of 2-3 min at RT samples were centrifuged for 15 min at 12.000 x g and 4°C (Eppendorf™ Centrifuge 5804, Eppendorf, Germany). During phase separation, the mixture separated into a lower red phenol-chloroform phase, an interphase, and a colorless upper aqueous phase containing the RNA. Only the supernatant (colorless upper aqueous phase) was removed cautiously and transferred into a new 1.5 ml RNase-free Eppendorf™ tube stored on ice. 50 µl nuclease-free water (Sigma-Aldrich, USA) was pipetted into the Precellys™ tubes containing the remaining phases, carefully inverted and vortexed, and centrifuged for 15 min at 12.000 x g and 4°C. Again the aqueous phase was removed cautiously and added to the first part of the aqueous phase into the 1.5 ml RNase-free Eppendorf™ tube. For precipitation, an equal volume of 100% molecular biology grade ethanol (AppliChem, Germany) was pipetted into the aqueous phase (1:1) and mixed accurately by inverting and vortexing. Afterwards, the precipitation product was transferred into a Zymo-Spin™ IC column with corresponding collection tube and centrifuged for 30 s at 12.000 x g (Eppendorf™ Centrifuge 5430, Eppendorf, Germany). The IC column was transferred into a new collection tube and the flow-through was discarded. 400 µl RNA Wash Buffer was pipetted to the IC column and after centrifugation for 30 s at 12.000 x g the flow-through was discarded again. For a DNase I treatment a mastermix of 5 µl DNase I + 35 µl DNA Digestion Buffer was prepared and stored on ice until further use. 40 µl of the set up mastermix were added directly to the column and incubated for 15 min at RT. Subsequent the column was washed two times by adding 400 µl Direct-zol™ RNA PreWash and after each addition the column was centrifuged (30 s at 12.000 x g) and flow-through was discarded. As a final washing step 700 µl RNA Wash Buffer was added, the column was centrifuged for 3 min at 12.000 x g and the flush-through was discarded. To achieve a complete clearance of RNA Wash Buffer a dry spin for 1 min at 13.000 x g was performed. Hereafter, the IC column was transferred into a 1.5 ml RNase-free Eppendorf™ tube and 15 µl of nuclease-free water was directly added to the column to elute the RNA. The column with eluate

was centrifuged (30 s at 12.000 x g) to collect the RNA in the Eppendorf™ tube underneath. Finally, the RNA was stored at -80°C for later analysis.

RNA concentrations and purity of brain and eyestalk tissues were determined by using the NanoDrop™ 2000 Spectrophotometer (Thermo Fisher Scientific, USA). In general, 260/280 ratios ~2.0 are accepted as 'pure' RNA, which means appreciably lower or higher values may indicate the presence of protein, phenol or other contaminants that absorb strongly at or near 280 nm. The 260/230 ratios represents a secondary measure which normally displays higher values than the respective 260/280 ratios, laying in the range of 1.8-2.2 for 'pure' nucleic acid. Following mean values could be determined for the examined tissues: eyestalk samples showed a mean 260/280 ratio of 2.09 and a mean 260/230 ratio of 2.26, while brain samples displayed a mean 260/280 ratio of 2.07 and a mean 260/230 ratio of 2.19. To test the integrity of extracted RNA and potential presence of leftover genomic contamination the Agilent Bioanalyzer 2100 (Agilent Technologies, Inc., USA) and the Agilent RNA 6000 Nano Kit were used (Fig. 7) according to manufacturer's instructions.

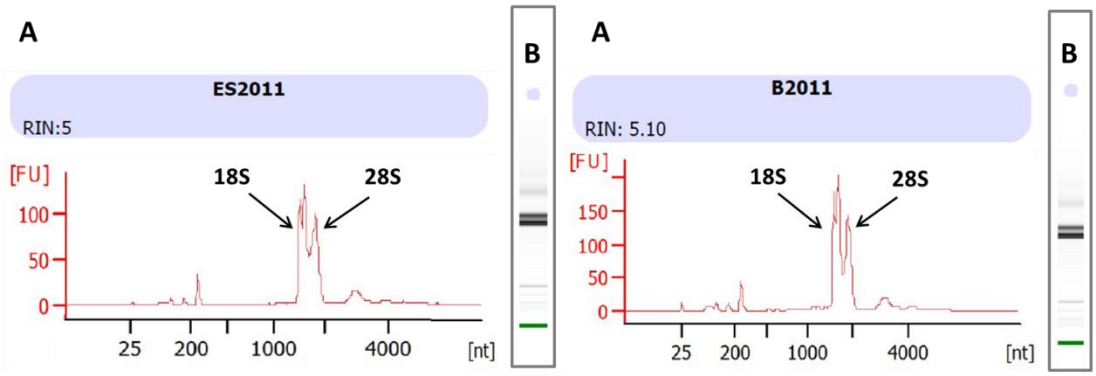

Figure 7: Electropherogram (A) and gel (B) of an exemplary eyestalk (left panel) and brain (right panel) sample of Antarctic krill (*E. superba*) - Results of a microfluidic electrophoresis performed in the Agilent 2100 Bioanalyzer using the RNA 6000 Nano Kit System. Time of RNA peak appearance (size related; x-axis) is plotted against the fluorescence (concentration related; y-axis). Small smudgy peaks within the 200 to 1000 nt region usually do indicate degradation, while big bulked peaks within the 2000 to 4000 nt region do indicate genomic contamination. RNA degradation and genomic contamination were not obvious, neither in the electropherogram (A) nor in the progress of the gel (B). The 18S peak resulted from the presence of 18S rRNA which is a component of the small eukaryotic ribosomal subunit, while the 28S peak resulted from the presence of 28S rRNA which is the structural ribosomal RNA for the large subunit of eukaryotic cytoplasmic ribosomes. These two characteristic peaks do suggest that the RNA which was analyzed came from a eukaryotic organism, in this case from the head section of Antarctic krill *E. superba*.

2.6 Preparation of spike controls

In this study in order to ensure an accurate normalization of gene expression, a combination of internal (housekeeper genes or HK) and external (spike) controls was used. In general, HK are usually constitutive genes, required for the maintenance of basic cellular functions, and are expressed in a rather constant level in all cells of an organism under normal conditions. The expression of one or multiple HK can be used as a reference for the analysis of expression levels of other genes. A chosen HK should be uniformly expressed with low variance across experimental conditions. The inclusion of HK into a RT-qPCR assay allows to correct for sample to sample variations in qPCR efficiency and errors in sample quantification. The HK has the advantage that it is not affected by technical errors (for example during cDNA preparation), however some residual biological variability might have an impact on it. For example, HK may show small fluctuations in gene expression over the 24 h. In contrast, an external target sequence control (spike) might be biased by some technical errors (for example during pipetting in the different cDNA samples), but it might not be affected by biological variability (same amount is added to all samples). Therefore, a combination of internal and external control seems to be a most accurate solution for gene expression normalization.

Six spikes were generated by cooperation partners at the Department of Biology at the University of Padua (Padua, Italy) and were selected from a human transcript plasmid library. Based on qPCR and efficiency results (Pitzschler, 2018), two spikes (hereafter denoted as spike 1 and spike 2) were chosen out of the six for further procedure.

2.6.1 Transcription of the spikes, purification, and quality control

For each spike, 3 µg dry pellet of linearized plasmids were re-suspended in 20 µl nuclease-free water by cautious vortexing. The spike suspensions were stored at 4°C overnight. After that, around 0.4 µg spike DNA were transcribed into RNA using the MAXIscript™ T3 Transcription Kit (Thermo Fisher Scientific, USA). For one transcription reaction 5 µl of MAXIscript™ mastermix (1 µl 10 x transcription buffer, 0.5 µl 10 mM ATP, 0.5 µl 10 mM CTP, 0.5 µl 10 mM GTP, 0.5 µl 10 mM UTP, 1 µl T3 enzyme mix, and 1 µl nuclease-free water) were pipetted together. 3 µl of re-suspended spike was filled up with 2 µl nuclease-free water and added to the 5 µl mastermix to achieve a final reaction volume of 10 µl. The mixture was pipetted gently up and down to ensure better mixing. Afterwards it was briefly centrifuged and incubated for 1 hour (h) at 37°C. 0.5 µl TURBO DNase™ was added, mixed

well, and incubated for further 15 min at 37°C. Subsequently, 40 µl nuclease-free water was added to reach a final volume of 50 µl. Transcripts were purified and cleaned with the RNA Clean & Concentrator^{TM}-5 kit (Zymo Research, USA). Therefore, 100 µl RNA Binding Buffer was added, mixed well and 150 µl 100% molecular biology grade ethanol (AppliChem, Germany) was enclosed and mixed well. Reaction mixture was transferred to a Zymo-Spin^{TM} IC column and centrifuged for 30 s at 12.000 x g. 400 µl RNA Prep Buffer was added to the column, centrifuged for 30 s at 12.000 x g, and flow-through was discarded. The procedure was repeated with 700 µl RNA Wash Buffer. 400 µl RNA Wash Buffer was added, centrifuged for 3 min at 12.000 x g, and flow-through was discarded. After that, a 'dry spin' for 1 min at 13.000 x g was performed to ensure the removal of RNA Wash Buffer. 8 µl nuclease-free water were directly added to the column and centrifuged for 30 s at 12.000 x g. Concentration and purity of the eluted RNA was measured by using the NanoDrop^{TM} 2000 Spectrophotometer, while integrity and presence of contaminants was checked with the Agilent Bioanalyzer 2100 (Fig. 8). After these analyses, the spike RNA was stored at -80°C.

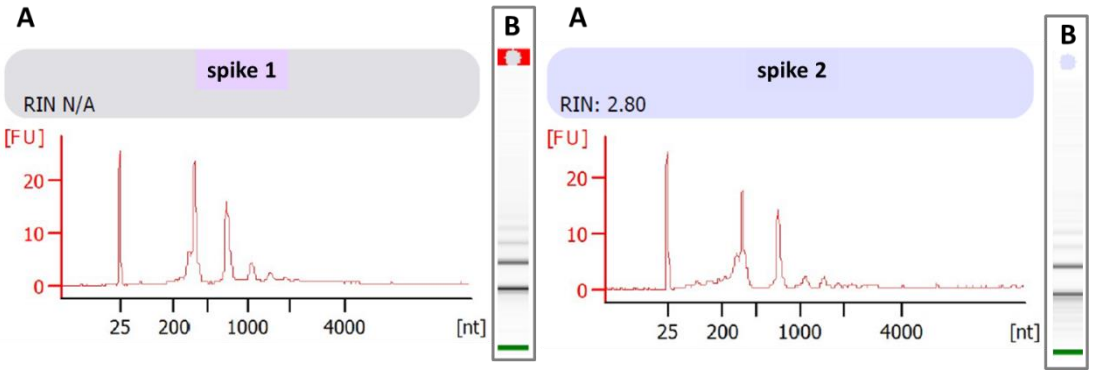

Figure 8: Electropherogram (A) and gel (B) of spike 1 (left panel) and 2 (right panel) for *E. superba* samples – Results of a microfluidic electrophoresis performed in the Agilent 2100 Bioanalyzer using the RNA 6000 Nano Kit System. Time of RNA peak appearance (size related; x-axis) is plotted against the fluorescence (concentration related; y-axis). The lower marker of the Kit System showed a peak at 25 [nt], while the spike displayed a peak around 220 [nt]. Both electropherograms revealed a similar peak pattern (750 nt, 1000 nt, 1800 nt). These peaks could be a result of non-completed DNA digestion, but they do not affect the analyses. For more accurate verification, sequencing would be required.

2.6.2 Determination of optimal spike concentration for further chronobiologic analyses

In order to determine the optimal concentration of spikes for further chronobiological examinations, we performed qPCR using different concentrations of the spikes (5 ng, 500 pg (0.5 ng), 50 pg, 5 pg, 1.4 pg and compared the resulting Ct values to those of the clock genes *Period* and *Cry2* (Fig. 9, see Appendix for detailed technical description). The clock genes *Period* and *Cry2* gave Ct values between 24 and 26 (Fig. 9B). Among spike concentrations, the one which was closer to these Ct values and could therefore be considered as optimal was 5 pg (Fig. 9A). Following the procedure, the optimal spike concentration must be added to each RNA sample before cDNA synthesis in the same amount. In order to reduce technical errors which might occur when pipetting low volumes, we decided to use for the final cDNA synthesis not 1 µl of the 5 pg spike dilution, but 5 µl of the 1.4pg dilution instead, which gave us a final spike concentration of approx. 7 pg, which was still optimal for our scopes.

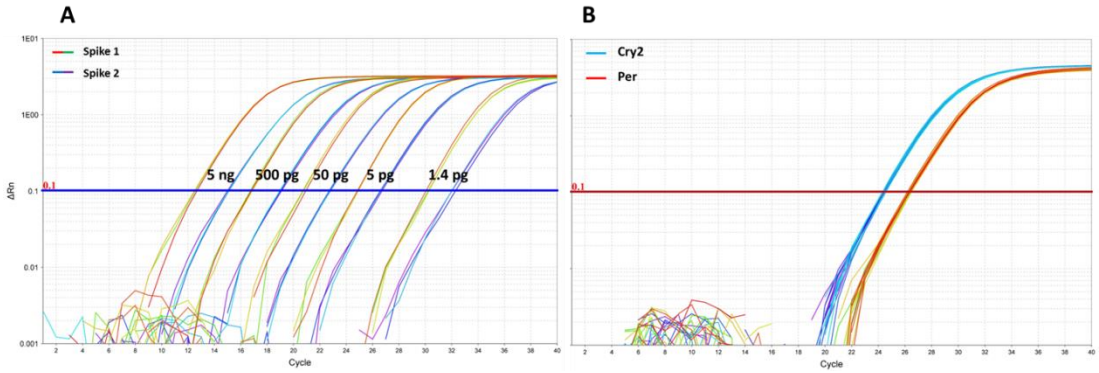

Figure 9: Amplification plots of the TaqManTM Real-Time PCR-Assay – A) Amplification plot of the spike controls 1 and 2 with different concentrations (5 ng, 500 pg, 50 pg, 5 pg, 1.4 pg). **B)** Amplification plot of the genes *Chryptochrome2* gene (*Cry2*) and *Period* (*Per*). Ct values of *Cry2* reached the threshold baseline (0.1) after approx. 24 cycles, while *Per* Ct values reached the baseline after approx. 26 cycles. The spike concentration (A) which corresponded most likely to this was above 5 pg. For further analyses 7 pg of spike1 and 2 were used.

2.7 cDNA synthesis of tissue-specific RNA extracts

Extracted RNA of brain and eyestalk samples from *E. superba* must be converted to cDNA for polymerase chain reaction. For one cDNA synthesis reaction 5 µl of the spike 1 and spike 2 mastermix (1.4 pg/µl x 5 µl = total amount of 7 pg/µl), 23.25 µl of RNA (1 µg RNA was diluted with RNase-free water), and 21.75 µl of mastermix (10 µl 5 x reaction buffer, 1 µl dNTPs (10 mM), 0.5 µl RNase Inhibitor (40 U/µl), 5 µl pentadecamere (500 µM), 0.25 µl Reverse Transcriptase and 5 µl RNase-free water; Thermo Fisher Scientific, USA) were pipetted together (total volume: 50 µl). NTCs and –RT controls were included on both cDNA synthesis plates. The two plates, one for the krill brain RNA and one for the krill eyestalk RNA were sealed, vortexed, and briefly centrifuged. RNA samples were reversely transcribed into cDNA using the T100™ Thermal Cycler (Bio-Rad, USA) under following conditions: 25°C for 10 min, 37°C for 50 min, and 70°C for 15 min. After synthesis the cDNA was stored at -20°C for further analyses. One biological replicate of the brain sample pool (#B_2027 at TP02) was excluded before cDNA synthesis as RNA concentration was too low. As a result only the following replicates of eyestalks and brain were reverse transcribed into cDNA and further used for gene expression analyses (ES: TP01 n=10; TP02 n=10; TP03 n=10; TP04 n=10; TP05 n=10, TP06 n=7 and for B: TP01 n=10; TP02 n=9; TP03 n=10; TP04 n=10; TP05 n=10, TP06 n=7).

2.8 Analysis of gene expression via TaqMan™ qPCR

2.8.1 Custom TaqMan™ Array Card Design

TaqMan quantitative reverse transcriptase-RT-PCR can be used to quantitate mRNA levels for selected genes and to increase the specificity of qPCR. The Custom TaqMan™ Array Card is a 384-well microfluidic card designed to perform 384 simultaneous real-time PCR (qPCR) reactions without using liquid-handling robots or multichannel pipettors to fill the card on the ports. This format allows for 1–8 samples to be run in parallel against 12–384 TaqMan™ Gene Expression Assay targets that are pre-loaded into each of the wells on the card. We chose the card format 16 (Fig. 10) with 16 gene expression assays (13 target genes + 1 internal control + 2 spike controls), 3 technical replicates per assay and 8 biological samples per card.

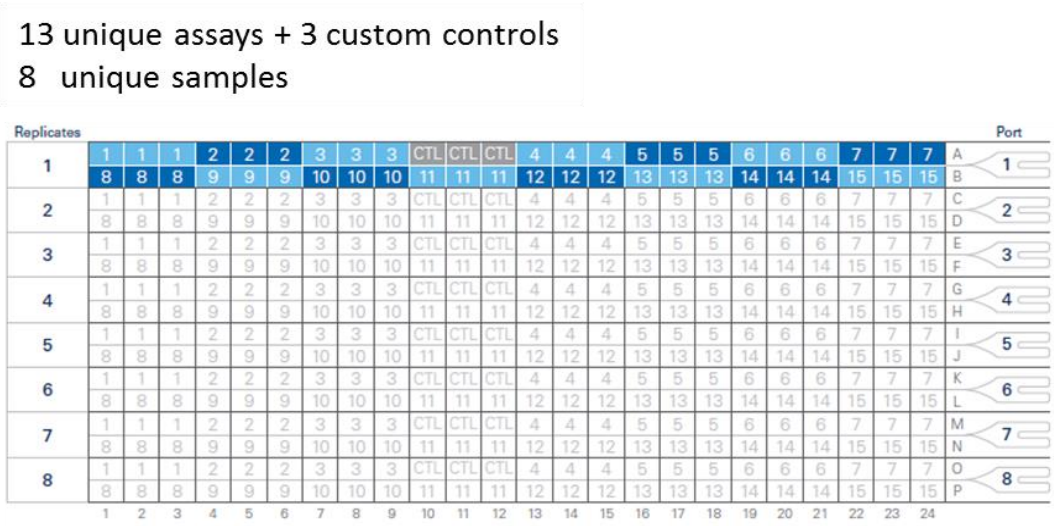

Figure 10: Custom TaqMan™ Array Card format with 13 unique assays and 3 custom controls used in this study – Instead of the mandatory control (CTL) slot 3 custom controls (internal: *Usp46* and external: spike 1 and 2) were loaded. The 8 unique samples were loaded using the ports on the right hand side. Modified. [Reference: https://assets.thermofisher.com/TFS-Assets/LSG/Warranties/cms_040127.pdf].

2.8.2 Gene selection for the Custom TaqMan™ Array Card

Based on published data (Hardin, 2009; Mazzotta *et al*., 2010; Teschke *et al.,* 2011; De Pittà *et al*., 2013; Tomioka and Matsumoto, 2015; Hunt *et al*., 2017) the regulatory genes *Clock (Clk), Clockwork orange (Cwo), Cryptochrome 2 (Cry2), Cycle (Cyc), Doubletime (Dbt), E75, Period (Per), Shaggy (Sgg), Timeless (Tim),* and *Vrille (Vri),* all involved in the essential regulatory loops of the insect circadian clockwork (Fig. 1) were selected as target genes together with the metabolic key enzyme *Adenosine triphosphate-γ (Atpg). Ubiquitin specific peptidase 46* (*Usp46*) was chosen as internal control (HK). This was based on previous studies (Biscontin *et al*., 2016, Piccolin *et al*., 2018a) which showed that the expression levels of *Usp46* were constant over the 24 h in different light:dark (LD) conditions. In addition to the internal control *Usp46*, two external spike controls (spike 1 and spike 2) were chosen (GenBank: spike1; XM_017004857.1 and spike 2; XM_011537537.1) (Tab. 2). Sequences of the named genes were acquired from the krill database available at http://krilldb.bio.unipd.it/ (Sales *et al.,* 2017), except for *Cry2* which can be accessed via GenBank (https://www.ncbi.nlm.nih.gov/genbank/). Moreover, since molecular investigations in krill clock genes are still at an early stage, we were interested in testing different primer sets. Hence, to determine the relative mRNA levels of the clock genes *Clock*, which is part of the positive heterodimer CLK-CYC,

and *Timeless*, which is part of the negative feedback loop TIM-PER, we used two different set of primers. One was used by Piccolin *et al*. (2018a) to investigate the plasticity of the clock in different photoperiodic conditions (denoted hereafter as *Clk_A* and *Tim_A*), while the other was used by Biscontin *et al*. (2017) to characterize the molecular functioning of the clock in krill (denoted hereafter as *Clk_B* and *Tim_B*) (Tab. 2).

Table 2: Primer sequences of target genes, housekeeping genes, and spike controls used for RT-qPCRs – Sequences of genes were obtained from the krill database (http://krilldb.bio.unipd.it/; Sales *et al.,* 2017) except for spike 1, spike 2 and *Cry2*, which can be accessed via GenBank (https://www.ncbi.nlm.nih.gov/genbank/).

Target gene		**Primer sequence (´5 -´3)**	**Accession number**
Clock_A	fdw	GGCCTCAGTTGGTACGAGAAATG	ESS034514
	rev	AATTTCCATTCTATACTGTGCCTTGATGT	
Clock_B	fdw	GCAGCGTCAGCTTCAAGAG	ESS034514
	rev	GCTGTTGTCGCATTATCATTTGCT	
Cycle	fdw	GCAGGATCAGATTGTGCGTCAA	ESS133965
	rev	TGCTATCTACACAGGAAGCTCTTCT	
Period	fdw	TGAGGGTAAATTCAACAATAAATGGAAT ACATCT	ESS133963
	rev	GAGTAACATCAACATTTTCCAACCAACT	
Timeless_A	fdw	CAAGACAAAGCGAGATGGCATTT	ESS040526
	rev	AGGGTTGGAAGAAGGTTTTGTGAAA	
Timeless_B	fdw	CAGCTTGTGCTCCATGGAAAAC	ESS040526
	rev	CTTAGGCAGTTGATGTAAGATCATGTCT	
Cryptochrome 2	fdw	CAGTGCTCAAGAACTTCCCAACTAA	FM200054,
	rev	GTCCTATGACACATTTAGACTGT	Mazzotta *et al*., 2010
Clockwork orange	fdw	AAAACTTTGATAAACAAAACCTCTTTCATC	ESS049812
	rev	GAGGGAGCTCATGACATGTGT	
Vrille	fdw	GAAGTAGCTACACTTAAATACCTGTTGGT	ESS123359
	rev	CAAAACTATTCTAACGAGATCCATCGGA	
E75	fdw	CAGTCTGCTTCTGCTTCAACCT	ESS094384
	rev	GCCTTCTGACGGTGCTCTAC	
Doubletime	fdw	AAAGAATAGAGCTTCAATATGTATATATTTAAAACAAAGT	ESS096455
	rev	TGAAAACAAGAAAAATTATAGAATCTTCTATCCTAGATAAGG	
Shaggy	fdw	GGTGGGTTGCGGAACATTG	ESS074789
	rev	TGGTCCACCACTGCCA	
Adenosine triphosphate-γ	fdw	GTCAAGAACATCCAGAAGATCACTCA	ESS108986
	rev	GCTTCAACTCCCTTTCAGCTCTT	
Housekeeping gene		**Primer sequence (´5 -´3)**	
Ubiquitin specific peptidase 46	fdw	TGGAACTGGTATTAACAGAGGACACT	ESS079224
	rev	CTGCATCGTCATCAAAGAGCA	
Spike control		**Primer sequence (´5 -´3)**	
Spike 1	fdw	TGCAATGATGATAACCGTTCCCTTTAA	XM_017004857.1
	rev	CCAGATATGCTTGAATTGGATCACCT	
Spike 2	fdw	GCTGGGACCTAGTGTCAAGTAC	XM_011537537.1
	rev	TGGAGTAACCATGCTAGATTAAAGAAATACAATT	

2.8.3 Primer design and sequence validation for Custom TaqMan™ Array Card

First, the selected target gene sequences (Tab. 2) for the Custom TaqMan™ Array Card were validated by using the Basic Local Alignment Search Tool (BLAST) of the National Center for Biotechnology Information (NCBI; https://www.ncbi.nlm.nih.gov) and the BLASTN and BLASTX search. Afterwards, chosen sequences were verified against the krill-specific sequences database (http://krilldb.bio.unipd.it/; Sales *et al.,* 2017). The reading frame of each target gene sequence was analyzed by using the web-based tool *Reverse complement* (https://www.bioinformatics.org/sms/rev_comp .html) and converted into its reverse counterpart in case of necessity.

A good primer design is essential for a successful qPCR reaction and many factors have to be taken into account when designing the optimal primers for target genes. Therefore low-complexity regions and interspersed repeats within the sequences were masked with the web-tool *RepeatMasker* (http://www.repeatmasker.org) to avoid primer cross-reactivity (self-dimers or primer-dimers) and mispriming. Finally, a 150 nucleotide long part without low-complexity regions and interspersed repeats which was located close to the 3'-end of each target sequence was selected and cut with the aid of *EMBOSS seqret* (http://www.ebi.ac.uk/Tools/sfc/emboss_seqret). For automatic primer design, the processed target sequences were then loaded into the Custom TaqMan™ Assay Design Tool from Thermo Fisher Scientific (https://www.thermofisher.com/order/ custom-genomic-products/tools/cadt). In general, a length of 18-30 nucleotides (or base pairs) for primers was favoured for adequate specificity and for an easy bind to the template at the annealing temperature. Besides, a GC base content of 40-60% was established, with the 3'end of a primer ending in C or G to promote binding and to guarantee an optimal primer melting temperature (T_m) for successful annealing. Afterwards, assay IDs were compiled and pasted into the format of the Custom TaqMan™ Array Cards (Fig. 10). For a detailed overview of primer sequences of chosen target genes, housekeeping genes, and spike controls used for the following TaqMan™ RT-qPCRs, see Tab. 2.

2.8.4 Primer efficiency for all primer sets (in particular for *timeless* and *clock)*

qPCR dilution series with the following cDNA concentrations: 100 ng, 200 ng, 400 ng, 800 ng were used to calculate primer efficiencies for all primer sets. *Threshold cycle* values (hereafter Ct-values) were plotted against the logarithm of the qPCR dilution series. For each dilution series a regression line with slope and intercept was calculated and mean Ct-values were plotted against the logarithmic

concentration. Values of the correlation coefficient (R^2) were close to 1 (0.9089 to 0.9993) for all primer pairs (Tab. 3 and Tab. 4, Appendix) indicating strong positive relationships between the variables. Moreover, efficiencies were calculated for each primer pair using the formula E = ($10^{(-1/slope)}$ -1) x 100. Based on empirical investigations, acceptable efficiencies in general should range between 90% and 110% with corresponding slopes between -3.1 and -3.6, (e.g. Ramakers *et al*., 2003; Rutledge and Côté, 2003; Hellemans *et al*., 2007). As efficiencies for *Sgg* in both tissues were below an acceptable range, we recommend utilizing different primers in the future.

Efficiencies for *Clk_B* and *Tim_B* primers were below the tolerable range in both tissues (brain: *Clk_B* = 69.1%, *Tim_B* =82.0%; eyestalks: *Clk_B* = 71.14%), as were the slopes (brain: *Clk_B* = -4.38, *Tim_B* = -3.84; eyestalks: *Clk_B* = -4.28) (see Fig. 11). In comparison, *Clk_A* and *Tim_A* primer pairs indicated better and in-range efficiencies in both tissues. In addition, the investigation of rhythmic gene expression gave better statistical results using the *Clk_A* and *Tim_A* primer sets than *Clk_B* and *Tim_B* (data not shown). Hence, *Clk_A* and *Tim_A* were used.

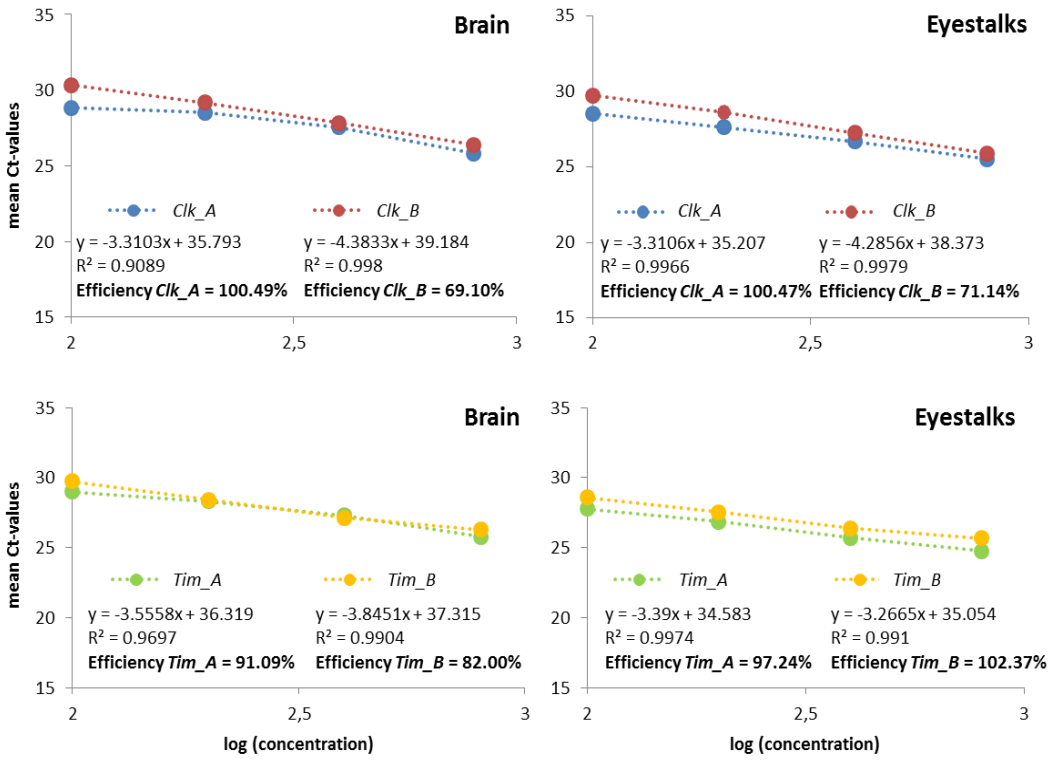

Figure 11: Primer efficiency using clock gene specific primer sets – Mean Ct-values of *Clk* and *Tim* primer sets were plotted against the logarithm of cDNA concentration used in a dilution series (100 ng, 200 ng, 400 ng, and 800 ng) in brain and eyestalks tissue, respectively. Primer efficiencies were calculated using the formula E= ($10^{(-1/slope)}$ -1) x 100. Efficiencies [%] for each primer pair within the respective tissues are indicated in bold.

2.8.5 qPCR with Custom TaqMan™ Array Cards

For the run of TaqMan™ Gene Expression Assays, 100 µl of total volume per reaction (20 µl of the respective cDNA (20ng/µl), 30 µl RNase-free water, and 50 µl TaqMan™ mastermix) was pipetted in a 1.5 ml Eppendorf™ tube. Tubes were briefly centrifuged and for each reaction, 98 µl were slowly added into the corresponding sample-loading port. Loaded TaqMan™ cards were centrifuged two times for 1 min at 1.200 rpm. Afterwards cards were inserted into the sealer, closed, and loaded-ports were removed using a scissor. The TaqMan™ cards were loaded into the ViiA™ 7 Real-Time PCR-System (Thermo Fisher Scientific, USA). Reaction conditions were as follows: one cycle of stage 1 which included 50°C for 2 min and 95°C for 10 min, followed by 40 cycles of stage 2 which included 95°C for 15 s and 60°C for 1 min.

2.8.6 Data quality control of TaqMan™ qPCR results

Following the TaqMan™ qPCR, amplification plots were checked via the ViiA™ 7 software to ensure that every reaction was done properly. All raw Ct-values above 32 were excluded, due to the general assumption that there might have been unspecific amplification. For each assay, we checked the technical replicates (triplicates) looking for consistency within Ct values. If calculated standard deviation among replicates was above 0.2, the replicate showing the Ct value most distant from the average was manually removed and the mean and the standard deviation were recalculated. In this way, it was possible to get the mean Ct values of at least 2 technical replicates per assay.

2.9 Normalization of raw Ct values and relative quantification of mRNAs

In this study, expression levels of target genes were normalized and quantified using the modified $2^{-\Delta\Delta Ct}$ method after Hellemans *et al*, (2007). This method takes the gene-specific amplification efficiency of the primers used into account and also allows for the combination of multiple reference genes during the normalization process. To determine the most stable combination of an internal and external HK to use for normalization procedure, raw Ct-values from all genes were evaluated with the software NormFinder (Andersen *et al*., 2004) in Microsoft Excel (2010). For both brain and eyestalks, the most stable combination was *Usp46* (internal HK) together with spike 1 (external HK), which was therefore used as reference in the normalization procedure (Fig. 12). The scaling of raw Ct-values (calculation of relative quantities; RQs) was accomplished for each tissue separately (brain and

eyestalks) as well as across the tissues. Normalized relative quantities (NRQs) were calculated by selecting as a baseline the sample showing the lowest Ct-value among both tissues

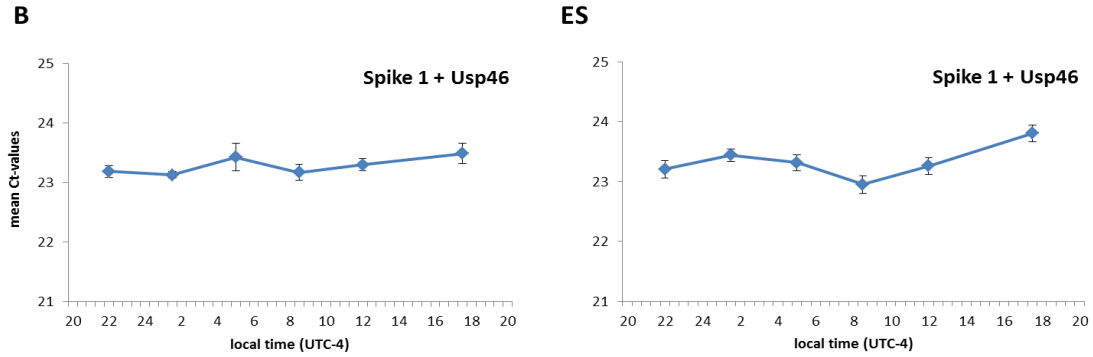

Figure 12: Geometric mean of raw Ct-values of internal and external control - UTC-4 = Coordinated Universal Time minus 4 hours, indicates the local time in Bransfield Strait, Antarctica at time of sampling. Raw mean Ct-values (y-axis) were plotted against the UTC-4 (x-axis). Left panel: Combination of Spike 1 + *Usp46*, respectively in brain. Right panel: Combination of Spike 1 + *Usp46*, respectively in eyestalks. Data are expressed as geometric mean ± SEM (brain: n= 10, 9, 10, 10, 10, 7; eyestalks: n= 10, 10, 10, 10, 10, 7).

2.10 Statistics

After normalization, NRQ values from all clock genes were examined for outliers using the Rosner Extreme Studentized Deviate test (EDS) for multiple outliers (two sided test) (Rosner, 1983). Rosner's outlier test requires a sample size of at least 25 (our study n=57) or greater and that data are normally distributed. The null hypothesis (H_0) for Rosner's outlier test was: There are no outliers in the data set. The significance level (*p*-value probability) was set low at α=0.01 to ensure not to exclude realistic data with individual biological variability. Additionally, TaqMan™ amplification plots of detected outliers were examined and outliers were kept if no abnormities spotted. In the end, no Ct values were excluded.

All statistical analyses were performed with the software RStudio (RStudio Team (2019) RStudio: Integrated Development for R. RStudio, Inc., Boston, MA). To illustrate hierarchical relationships among daily gene expression patterns of tested clock genes in the different tissues, the R package gplots (Warnes *et al*., 2019) was used to generate heat maps and dendrograms. First, in order to make the range of

gene expression variation comparable for all genes, NRQ values were transformed to Z-values with the formula:

$$\text{function}\,(x)(x - \min(x))/(\max(x) - \min(x)$$

Then data were clustered using Euclidean distance and Ward's linkage, as this often provides strong clustering results in practice. The package RColorBrewer (Neuwirth, 2014) was used to implement a color-coded scale, where blue represents high and yellow low expression levels, respectively. To test the statistical significance of the clusters put in evidence by the dendrograms, a hierarchical cluster analysis was conducted using the R package sigclust2 (Kimes, 2018).

The RStudio package RAIN (Rhythmicity Analysis Incorporating Non-parametric Methods, Thaben and Westermark, 2014) was used to identify putative rhythmicity within a range of periods included between 12 h and 24 h in daily patterns of gene expression. We tested for this range of periods to ensure a detection of all rhythmic circadian behavior, including potential bimodal patterns with 12 h. For brain and eyestalk tissues, data were fit to sinusoidal curves with the required period. Within this curve the probability of consistency was expressed as *p*-values indicating the likelihood of the fit and the phase of the fitted curve, corresponding to the time point where the amplitude of the oscillation is maximal. Subsequently, *p*-values were corrected for multiple comparisons using the *false discovery method* (*fdr*) of Benjamini, Hochberg, and Yekutieli (Benjamini and Hochberg, 1995; Benjamini and Yekutieli, 2001) implemented within the package. To compare gene expression levels between eyestalk and brain tissues for each time point (TP01-TP06), the non-parametric Wilcoxon Rank Sum test implemented by the *wilcox.test* function in R was applied.

3 Results

3.1 Regulatory network of clock gene expression patterns

To visualize potential relationships among daily patterns of clock gene expression in brain and eyestalks tissue of *E. superba*, we used hierarchical clustering. By means of hierarchical cluster analysis the statistical significance of the groupings was verified. In brain, daily mRNA expression patterns were clustered within two separated groups consisting of (i) *Cyc, Cry2*, *Cwo*, *Clk*, and *Per*, as well as (ii) *Dbt*, *Tim*, *Vri*, and *Sgg* (Fig. 13A). Hence, the dendrogram (i) comprises core clock genes (*Cyc, Clk*) plus core clock gene regulators (*Cry2, Per*) and the associated clock gene *Cwo*, while the dendrogram (ii) contains the core clock gene regulator *Tim* plus kinases (*Sgg, Dbt*) and the associated clock gene *Vri*. The gene expression patterns of the associated clock gene *E75* and the metabolic gene *Atpg* did not align with the other groupings and form separate branches. A cluster analysis revealed no significant differences between the mentioned groups. In addition to a putative gene expression similarity, the heat map visualized the highest expression levels for *Cwo* at TP03 and TP06, for *Per* at TP01 and TP06, for *E75* at TP02, and for *Atpg* at TP04 and TP05, while the remaining eight clock genes showed highest expression levels at TP06, which representing the first time point after dusk at 17:30 local time (UTC-4), (Fig. 13A).

The clustering of the daily gene expression patterns recorded in eyestalks differs in some aspects from those in the brain. Here, the clustering revealed the following separated groupings: (i) *Cyc*, *Clk*, and *Tim*, (ii) *Cwo*, *Vri*, and *Sgg*, (iii) *Cry2*, *Per*, and *Dbt,* (Fig. 13B). Thus, the dendrogram (i) includes the core clock genes *Cyc* and *Clk,* plus the core clock gene regulator *Tim*, while dendrogram (ii) contains the associated clock genes *Cwo* and *Vri* plus the kinase *Sgg*. Dendrogram (iii), on the other hand, comprises the core clock gene regulators *Cry2* and *Per* plus the kinase *Dbt.* Furthermore, a cluster analysis revealed that the differences between the dendrogram (iii) and the dendrograms (i) and (ii) are significant (p-values < 0.05). The associated clock gene *E75* and the metabolic gene *Atpg* form separate branches just like in brain, however, the differences to the other dendrograms (i, ii, iii) are significant (p-values < 0.05). Similar to brain, most clock genes in eyestalk tissues had their highest expression peaks at TP06 after dusk. However, *Atpg* and *E75* showed highest expression peaks during night-time and sunrise (*Atpg*: TP03 and TP04, E75: TP02 and TP03), (Fig. 13B). Additionally, slightly elevated expression levels for all genes were noted at TP02 during night-time.

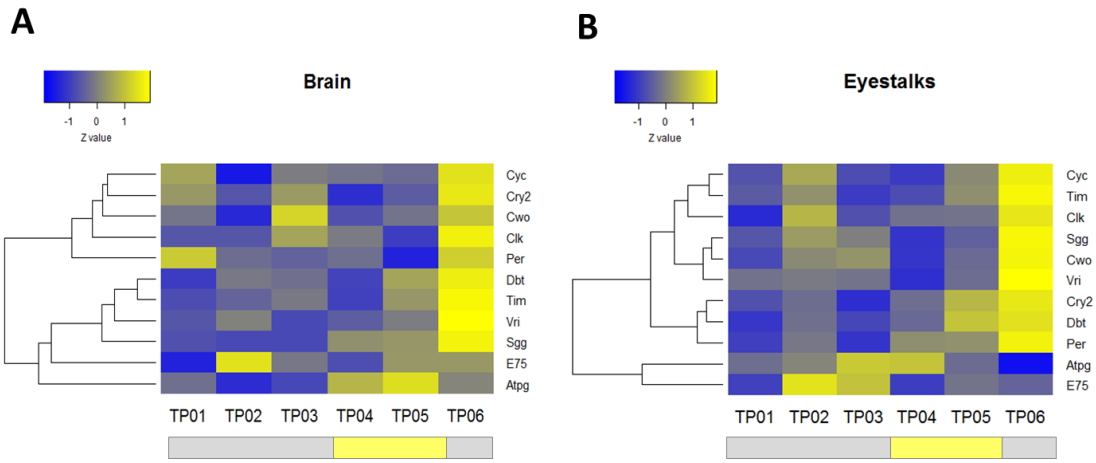

Figure 13: Heat maps of daily clock gene expression patterns in different tissues – A) Gene expression over time (24 h) in brain. **B)** Gene expression in eyestalks over time (24 h) (for more details concerning clock gene regulatory network see Figure 1). Heat maps and dendrograms show the expression levels of clock genes during the 24 h cycle and are represented with a color-coded scale; yellow and blue represent high and low expression levels, respectively. TP= time point, indicates the time point of sampling every 3.5 h in a time period of 24 h (except for TP06, it was 53.5 h). Genes clustered together based on similarity of daily gene expression patterns. Light bar beneath the graphs shows the respective photoperiod at the sea surface (grey = dark phase; yellow = light phase).

3.2 Daily profiles of clock gene expression in brain and eyestalks

The normalized clock gene expression levels (mean NRQ) in the two different tissues were plotted against local time in Bransfield Strait (UTC-4) and time points to illustrate the daily patterns in the 24 h cycle (Fig. 14 and 15). In addition, any statistical significant rhythmicity in brain or eyestalk tissues is presented for the respective genes. Moreover, any statistical significant differences between brain and eyestalk tissues per time point are described for the respective genes.

3.2.1 Analyzed differences within brain and eyestalks tissues

Brain

The daily gene expression levels in brain tissue for the core clock genes *Clk* and *Cyc* showed a similar pattern (Fig. 14). *Clk* and *Cyc* displayed a first expression maximum at night-time (TP03, 1.10 and 1.17, respectively). During the day (TP04-TP05), only expression levels in *Clk* decreased to 0.96. After mid-day (TP05), both core clock genes peaked after dusk (TP06, *Clk*: 1.20, *Cyc*: 1.23).

Similar expression patterns to that of core clock genes were found for the core clock gene regulators *Per*, *Tim*, and *Cry2* (Fig. 14). For the gene *Per*, the mean expression levels were relatively constant over the 24 h cycle ranging from 1.02 to 1.16, with a slight rise after mid-day (TP05) as already detected in the core clock gene *Cyc*. The expression patterns observed for *Tim* and *Cry2* were very similar to those of the core clock gene *Clk*. At night-time (TP01-TP03), all three expression patterns peaked before sunrise (TP03), followed by a slight decrease afterwards (TP04-TP05), and an overall increase during the day to highest expression levels after dusk (TP06, *Tim*: 1.30, *Cry2*: 1.10, *Cyc*: 1.23). In all core clock genes and their regulators, no significant rhythmicity was detected.

The associated clock gene kinases *Dbt* and *Sgg* showed no expression level patterns according to the ones observed in the core clock genes and their regulator genes (Fig. 15a). However, during night-time, expression levels of *Dbt* and *Sgg*, were constant, started to increase with sunrise (TP04) and peaked after dusk (TP06, *Dbt*: 1.08, *Sgg*: 1.47). A significant daily oscillation with a period of 24h was detected for *Sgg* (p=0.0007, Tab. 5; appendix).

For the associated clock genes *Cwo* and *Vri*, similar expression patterns to that of core clock genes (*Clk*) and regulators (*Cry2*) could be demonstrated. Mean expression levels of *Cwo* decreased at night (TP02, 0.88), increased before dawn to a first maximum (TP03, 1.18) and rose with sunrise (TP04) to the highest peak after dusk (TP06, 1.15). *Cwo* displayed similar expression levels like *Cry2* but with greater amplitude (Fig. 14 and 15b). The expression pattern of the associated clock gene *Vri* showed the same tendency as the pattern of the core clock gene *Clk* (Fig. 14 and 15b). Both exhibited constant expression levels during night-time, followed by an increase during dawn (TP03-TP04) and throughout the day to the highest peak after dusk (TP06, 0.92).

Mean expression levels of the associated clock gene *E75* remained constant and exhibiting their highest peak during night-time at TP02 (0.59) and not after dusk, showing no similarities to the other tested clock genes (Fig. 15b).

For the metabolic gene *Atpg* mean expression levels ranged from 0.65 to 0.80, whereby the lowest peak was detected during night-time (TP02, 0.65) followed by a slight increase (Fig. 15c). Afterwards, expression levels decreased at dawn (TP04) to 0.72 after dusk at TP06. The expression pattern was also not similar to other tested clock genes in this study.

Eyestalks

Daily gene expression levels in eyestalk tissues of the core clock genes *Clk* and *Cyc* showed a similar pattern, with a first peak at TP02 (*Clk*: 0.96, *Cyc*: 1.09), (Fig. 14). They re-increased throughout daytime (TP04 to TP05) to a maximum level after dusk (TP06, *Clk*: 1.08, *Cyc*: 1.18). A significant daily rhythmicity with a period of 16 h was detected in *Cyc* (p=0.048, Tab. 6, Appendix).

Similar gene expression patterns to those of core clock genes (*Clk*, *Cyc*) could be shown for the core clock gene regulators *Per*, *Tim*, and *Cry2* (Fig. 14), where *Tim* displayed the greatest amplitude and a significant daily oscillation with a period of 24 h (p=0.034, Tab. 6; appendix).

For the associated clock gene kinases *Dbt*, similar gene expression patterns to that of the core clock gene regulators were detected (Fig. 14 and 15a). *Dbt* showed the same expression pattern as *Per* with an increase during dawn and a peak after dusk (TP06, 0.89), whereby the amplitude was smaller. The mean expression levels of the associated clock gene kinase *Sgg* increased during night-time (TP02-TP03), decreased at sunrise (TP04, 1.04) and increased again after sunrise to peak after dusk (TP06, 1.56). Besides, *Sgg* exhibited a significant daily rhythmicity with a period of 16 h (p=0.008, Tab. 6, Appendix).

The expression patterns for the associated clock genes *Cwo* and *Vri* showed a similar tendency, but no similarities to expression patterns of core clock genes or regulators (Fig. 14 and 15b). However, a similar pattern as in the kinase *Sgg* could be observed for *Cwo* (Fig. 15a,b). *Vri* showed constant expression levels during night-time (TP01-TP03), followed by a decrease at sunrise (TP04, 0.70), and an increase after dusk to 1.11 at TP06, (Fig. 15b).

For the associated clock gene *E75* the mean expression levels increased from TP01 to highest peaks at TP02 and TP03 (1.06 or 0.99), followed by an abrupt decrease during sunrise (TP04, 0.69), and a slight constant increase afterwards until dusk (0.78, TP06), (Fig. 15b). There were no similarities to other tested clock genes.

The mean expression levels observed for the metabolic gene *Atpg* displayed a constant pattern during the night (TP01-TP03) followed by a decrease from 0.99 during dawn (TP04) to 0.76 after dusk at TP06 (Fig. 15c). Moreover, *Atpg* showed a significant daily oscillation with a period of 24 h (p=0.008, Tab. 6; appendix).

3.2.2 Analyzed differences between brain and eyestalks tissue

For all genes analyzed, mean expression levels at each time point (TP) were compared between brain and eyestalks to analyze significant differences (see Fig. 14 and 15 and Tab. 7, Appendix). In general, mean expression levels in *Clk*, *Tim, Dbt*, *Cwo, and Vri* displayed no significant differences between tissues. However, for *Cyc*, *Per*, *Cry2*, *Sgg, E75,* and *Atpg* significant variations could be demonstrated between brain and eyestalks (Fig. 14 and 15).

When compared to eyestalk tissues, the mean expression levels in brain were significantly higher over the first half of the time series during the night in the core clock gene *Cyc* (TP03, p=0.005) and in the regulators *Per* and *Cry2* (TP01: *Per* p=0.012, *Cry2* p=0.023; TP02: *Per* p=0.013, *Cry2* p=0.022; TP03: *Per* p=0.001, *Cry2* p=0.005), but also at dawn in the kinase *Sgg* (TP04 p=0.009), (Fig, 14 and 15a).

When compared to brain, mean expression levels in eyestalk tissues were significantly higher during night-time and dawn in the kinase *Sgg*, in the associated clock gene *E75*, and in the metabolic gene *Atpg* (*Sgg*: TP02 p=0.008, *E75*: TP01 p=0.012, TP02 p=0.030, TP03 p=0.025, TP04 p=0.015, *Atpg*: TP02 p=0.004, TP03 p=0.002, TP04 p=0.021), (Fig. 15a,b,c).

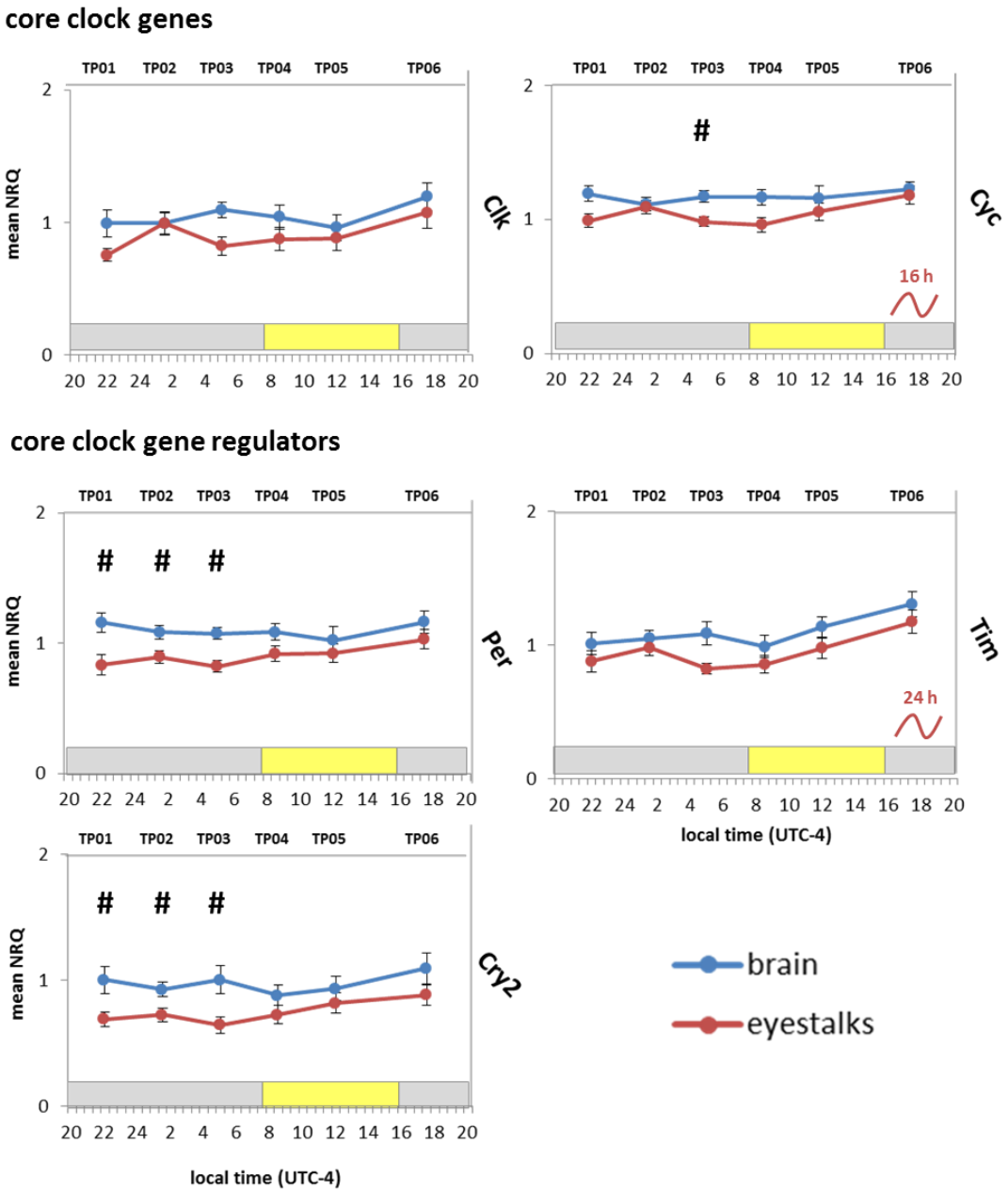

Figure 14: Core clock gene expression patterns in brain and eyestalks – Ten clock genes (*Clk, Cry2, Cwo, Cyc, Dbt, E75, Per, Sgg, Tim*, and *Vri*) and the metabolic key enzyme *Atpg* were analyzed over 24 h. Relative mRNA levels (NRQ) were plotted against local time (UTC-4). UTC-4 = Coordinated Universal Time minus 4 hours, indicates the local time in Bransfield Strait, Antarctica at time of sampling. Data are expressed as mean ± SEM (brain: n= 10,9,10,10,10,7; eyestalks: n= 10,10,10,10,10,7). TP= time point, indicates the time point of sampling every 3.5 h in a time period of 24 h (except for TP06, it was 53.5 h). Light bar beneath the graph shows the respective photoperiod (grey = dark phase; yellow = light phase) at the sea surface. Schematic sinus curves indicate significant daily oscillation for *Cyc* and *Tim* with a period of 16 h and 24 h in eyestalks determined by RAIN analysis (for *p*-values see appendix) in brain and eyestalks. Hash keys indicate significant differences between both tissues tested for each ZT (Whitney-Wilcoxon test).

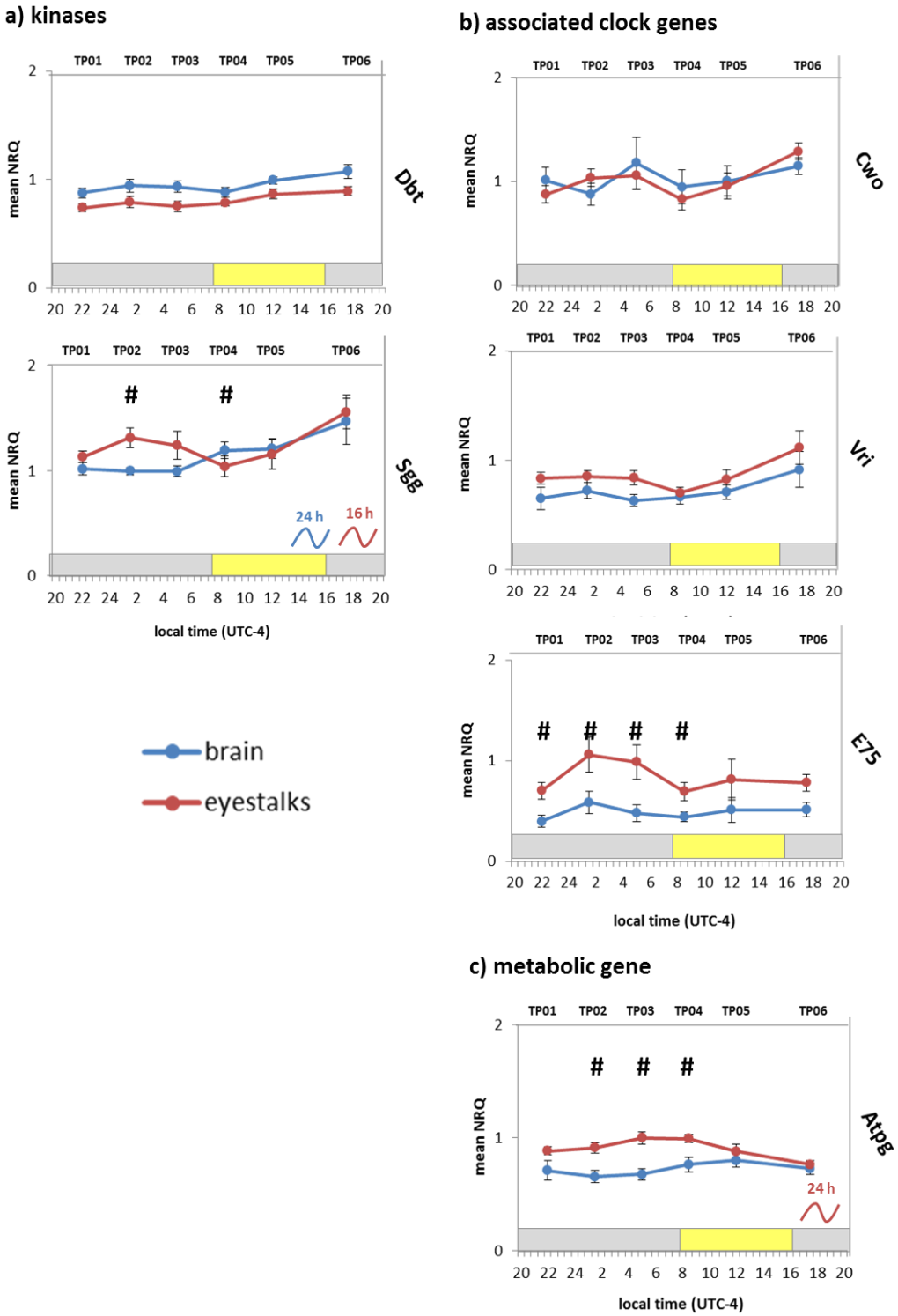

Figure 15: Associated clock genes and metabolic gene expression patterns in brain and eyestalks – Ten clock genes (*Clk, Cry2, Cwo, Cyc, Dbt, E75, Per, Sgg, Tim*, and *Vri*) and the metabolic key enzyme *Atpg* were analyzed over 24 h. Relative mRNA levels (mean NRQ) were plotted against local time (UTC-4). UTC-4 = Coordinated Universal Time minus 4 hours, indicates the local time in Bransfield Strait, Antarctica at time of sampling. Data are expressed as mean ± SEM (brain: n= 10,9,10,10,10,7; eyestalks: n= 10,10,10,10,10,7). TP= time point, indicates the time point of sampling every 3.5 h in a time period of 24 h (except for TP06, it was 53.5 h). Light bar beneath the graph shows the respective photoperiod (grey = dark phase; yellow = light phase) at the sea surface. Schematic sinus curves indicate significant daily oscillation with a period of 24 h for *Sgg* and *Atpg* in brain and eyestalks, respectively and a daily oscillation with a period of 16 h for *Sgg* in eyestalks. Hash keys indicate significant differences between both tissues tested for each ZT (Whitney-Wilcoxon test).

4 Discussion

The knowledge about an endogenous timing system in the Antarctic krill, *E. superba*, which controls metabolic and physiological output functions, has been augmented by findings of recent studies (Mazzotta *et al*., 2010; Teschke *et al*., 2011; de Pittà *et al*., 2013; Biscontin *et al*., 2017; Piccolin *et al*., 2018a; Höring *et al*., 2018; Pitzschler, 2018). In the present study, an attempt was made to identify potential circadian clock gene expression patterns (*Clock*, *Cycle*, *Period*, *Timeless*, *Cryptochrome2*, *Doubletime*, *Shaggy*, *Clockwork orange*, *Vrille*, *E75,* and the metabolic gene *Atpg*) in field samples from winter, thus adding important information to the rare winter data. Besides, methodological modifications were applied to reduce gene expression variability and to improve the detection of potential oscillation patterns in krill.

4.1 Environmental conditions in the field

In the Southern Ocean ecosystem, environmental factors such as food availability, sea ice extent, day length, and light intensity show extreme seasonal changes, which can affect the biological clock system in krill (Mazzotta *et al*., 2010). Moreover, abiotic and biotic environmental parameters of krill habitat in the Southern Ocean might be profoundly altered by global warming related to climate change (Smetacek and Nicol, 2005; Clarke and Harris, 2003). In this context, it is important to know the environmental conditions under which field krill were sampled for this study.

Light conditions at fishing depth

Perhaps the most important environmental cue for the entrainment of the circadian clock in krill and therefore for the regulation of metabolic and physiological output functions (e.g. DVM) is the occurring light regime, whereas recent studies also suggested a major influence of the light spectral composition (Mazzotta *et al*., 2010). For this study wild krill were sampled at 170 m depth, where irradiance was very low and maybe absent (Tab. 1). In contrast to the late-winter light regime at the surface, exhibiting 8 hours of light and 16 hours of darkness (LD 8:16) with irradiance of approx. 2 W/m² during night-time and approx. 20 W/m² during day-time, the calculated irradiance in 170 m depth was around 0 W/m². Studies on the visual capabilities of Antarctic krill are lacking (Frank and Widder, 1999), despite evidence that these species perform visually-mediated behaviors, such as DVM (Gaten *et al.,* 2008; Sourisseau *et al*., 2008). Hence, due to the putative vertical movements of krill

during the 24 h cycle, it is difficult to say at which depth krill were located before sampling. It can only be concluded, that all sampled animals were in the darkness at least from sunset to sunrise. The actual light exposure during the day might have been different for each individual sampled krill, and might vary between near-constant darkness (if the krill remained at or moved below the fishing depth at all times) and the photoperiod measured at the surface (if the krill spend most of the time close to the surface).

Krill abundance and chl *a* concentration

In general, krill concentrations and chl *a* concentration within the sampling area of Bransfield Strait (Tab. 1) were similar to the patterns observed for late-winter in previous years (Cleary *et al*, 2016; Reiss *et al*., 2017). The observed major differences in krill abundance between time points and therefore between sampling locations (Tab. 1) could be explained by DVM in krill or by a potential winter twilight DVM pattern between 100 to 350 m depths. Twilight DVM involves emerging towards the surface at sunset, a submerging to deeper water layers around midnight ('midnight sink'), followed by a second emerging towards the surface and then submerging again to deeper water layers at sunrise (Cohen and Forward, 2005). The abundance of sampled krill in a depth of 170 m might have been so different, due to the occurring migratory patterns of the crustaceans. In the sampling week August 7-13th, krill biomass formed a nearly continuous band (more than 64 kilometers) with distinctly different patterns of aggregation between daytime (compact dense swarms, 40 to 400 meters) and night time (broader patches between 0 and 200 meters) on several transects across Bransfield Strait (content block NBP1606 cruise, data not shown). Within Bransfield Strait, the lack of ice shield (Tab. 1) has kept crabeater seal abundance very low, while Antarctic fur seals are hauling out on the ice and snow free beaches rather than staying in the water, which potentially minimized the risk of predation (content block NBP1606 cruise, data not shown).

4.2 Regulation of clock genes in *E. superba* during winter conditions

In the regulatory network of clock genes within this study, some of them showed similarities in their expression patterns (Fig. 13, 14, and 15) and significant daily oscillation (Fig. 14 and 15) during a 24 h cycle.

The daily mRNA levels for the core clock genes *Clk* and *Cyc* showed synchronized expression in brain and eyestalks of *E. superba* within this study, with a first peak at

night-time and an upregulation during the light phase to maximum expression levels after dusk (Fig. 13 and 14). For *Clk*, no rhythmicity or significant differences were observed. This was also not the case in previous studies under controlled laboratory late-winter light conditions (Piccolin *et al*., 2018a). In addition, studies of thoracic ganglia and eyestalk nervous tissues in crustaceans also assumed a lack of a circadian rhythmicity within *Clk* mRNA expression (Strauss and Dircksen, 2010). Hence, our data also suggest that *Clk* might not display endogenous oscillatory rhythmicity in krill. However, for wild krill in summer a rhythmic 24 hour-oscillation of *Clk* was demonstrated, which could be a special adaption to the conditions during midnight sun in Antarctic summer (Biscontin *et al*., 2017). A significant rhythmic 16 hour-oscillation of *Cyc* mRNA expression could be identified in krill eyestalks (Fig. 14). Rhythmic oscillations in mRNA levels of *Cyc* have already been shown in krill eyestalks, but with a period of 24 h under LD 12:12 (Biscontin *et al.,* 2017; Pitzschler, 2018; Piccolin *et al*., in prep.). An explanation for the shift in the rhythmic of field samples could be the different light regime (approx. LD 8:16) together with environmental cues. Alternatively, this could be a hint for a putative 4 hour shifted bimodal pattern (Tessmar-Raible *et al*., 2011) which was also found in enzyme activity (Teschke *et al*., 2011) and in transcription patterns (de Pittà *et al*., 2013).

Both, the core clock gene regulator *Per* and the core clock gene *Cyc* displayed similar expression patterns in the brain with small amplitudes. However, the expression patterns observed for the other core clock gene regulators, *Tim* and *Cry2*, were very similar to those of the core clock gene *Clk*, with a peak at night-time and highest expression levels after dusk (Fig. 14). In contrast to previous studies of insects and crustaceans (Tomioka and Matsumoto, 2015; Sbragaglia *et al*., 2015; Zhu *et al.,* 2008), synchronized expression of *Per* and *Tim* could not be detected in the brain of krill. This is in line with the results of former laboratory krill studies (Pitzschler, 2018). A synchronized expression of *Cyc*, *Clk*, *Cry2*, and *Per* was identified in brain, whereas for eyestalks, a synchronized expression of *Cyc*, *Clk,* and *Tim* as well as *Per* and *Cry2* was found (Fig. 13). Negative (*Per*, *Tim*, *Cry2*) and positive (*Clk*, *Cyc*) clock components showed similar daily patterns in both tissues but an antiphase relationship between positive and negative clock components as in the *Drosophila* circadian feedback loop was not present in winter field krill (Dunlap, 1999; Hardin, 2005). Interestingly, the expression levels of *Cry2* in brain and eyestalks expressed no circadian rhythmicity as detected for krill in the laboratory (Teschke *et al*., 2011) and also for krill in the field during summer (Mazzotta *et al*., 2010; de Pittà *et al*., 2013). One explanation might be the different light regimes krill were exposed to, and beyond that other investigations did also not found circadian

WIE waren denn bei diesen Studien die Lichtverhältnisse

rhythms in *cry2* expression levels (Pitzschler, 2018; Höring *et al.*, 2018). Besides, *Tim* displayed a significant rhythmic 24 hour-oscillation in eyestalks, which was also observed in the Norwegian lobster *Nephrops norvegicus* (Sbragaglia *et al*., 2005) and in field krill during summer (Biscontin *et al*., 2017).

The associated clock gene kinases *Dbt* and *Sgg* showed no expression patterns comparable to the ones observed for the core clock genes in krill brain and eyestalks (Fig. 14 and 15a). However, a significant rhythmic 24 hour-oscillation was ascertained for *Sgg* in brain together with a significant rhythmic 16 hour-oscillation in eyestalks (Fig. 15a). In the circadian clocks of *Drosophila* (Allada and Chung, 2010) and krill (Biscontin *et al*., 2017), *Sgg* is responsible for the phosphorylation of *Tim* on the protein level to regulate the nuclear entry of TIM and PER. Based on this assumption, it could be presumed that the significant oscillation of *Sgg* and *Tim* might be related to each other. The kinase *Dbt* and the negative regulators *Per* and *Cry2* showed synchronized expression patterns in krill eyestalks (Fig. 13A), with an increase during dawn and a peak after dusk (Fig. 14 and 15a). In krill and *Drosophila*, DBT is identified to control nuclear entry of PER through phosphorylation while CRY2 is associated with PER as an additional negative regulator (Biscontin *et al*., 2017; Tomioka and Matsumoto, 2015; Mackey, 2007).

The metabolic gene *Atpg* showed expression pattern which were not similar to other tested clock genes in this study (Fig. 15c). In addition, *Atpg* showed a significant circadian 24 hour-oscillation in eyestalks. These significant oscillation patterns have already been investigated in wild krill (de Pittà *et al*., 2013) and under laboratory late-winter conditions (Piccolin *et al*., 2018b; Höring *et al*., 2018). Overall, no agreement in mRNA expression patterns could be detected in this study.

The associated clock genes *Cwo* and *Vri* showed synchronized expression (Fig. 13) with similar patterns to those of core clock genes (*Clk*) and regulators (*Cry2*) in krill eyestalks, but were not expressed in a circadian rhythm (Fig. 14 and 15b). In contrast, the associated clock gene *E75* displayed no similarities to other tested clock genes (Fig. 15b). However, circadian rhythmicity for *Cwo* and *E75* was identified in *Drosophila* (Matsumoto *et al.,* 2007; Kumar *et al*., 2014) but not in krill (Pitzschler, 2018), while a 24 hour-oscillation for *Vri* was observed in krill (Pitzschler, 2018). Possible explanations for the differences in the results could be: i) gene regulation in the fruit fly might occur in a different manner compared to krill, ii) an identification of clear oscillation patterns was not possible, although they were present, iii) functional participation of *E75* in the circadian clock of krill is still arguable iv) this study examined winter field samples and thus a direct comparison to a laboratory set up is not possible (Pitzschler, 2018).

In summary it can be stated that the relative mRNA levels of the clock genes from winter field krill samples analyzed within this study showed less pronounced or different patterns compared to findings for arthropods and in other krill studies. Additionally, correlations are more pronounced between clock genes in eyestalks compared to clock genes in brain. Similar findings in the literature lead to the assumption that krill eyestalks are good candidates for the search of genes involved in circadian regulation (clock genes) and for clearer results regarding temporal pattern of expression. However, it must be noted that the amplitudes of the clock genes were quite low and it is therefore difficult to draw conclusions about circadian rhythms of clock genes in wild krill used in this study. Those clock genes may have been subject to different regulatory mechanisms, forasmuch an identification of putative circadian rhythmicity was not possible. In addition, comparison of the present field results to data resulting from laboratory findings (even with late-winter regimes) or to data resulted from summer field findings must be considered with caution.

Warum denn empfehlen den ganzen Kopf zu nehmen

Despite all differences with previous studies and low amplitudes, significant rhythmicity for three clock genes (*Cyc*, *Tim*, *Sgg*) under very poor light conditions in sampling depths could be detected in krill sampled during late-winter. This suggests the assumption that krill clock functions might not be turned off at that time of the year. In addition, the difficulties related to the detection of rhythmicity might be partly due to the varying light conditions, which might have been experienced during the day by the individual krill while moving up and down in the water column.

Widerspruch zum Absatz davor?

4.3 Comparison of clock gene expression levels in brain and eyestalk tissue

Circadian rhythmicity in crustaceans is controlled by multiple sites of independent circadian pacemakers, including the retinae of the eye, the eyestalks, the supraoesophageal ganglion (brain) and the caudal photoreceptor which have already been verified as important parts in circadian regulation (Strauss and Dircksen, 2010; Aréchiga and Rodríguez-Sosa, 2002). Moreover, it has been shown that the presence of brain photoreceptors for light entrainment is both necessary and sufficient, but the important endogenous rhythm generator likely resides in the eyestalks (Strauss and Dircksen, 2010). To date, studies of transcriptional-level interactions between these tissues in krill and other crustaceans are scarce, possibly due to the need for complex dissection of both tissues (Pitzschler, 2018). Comparisons of relative mRNA levels for krill brain and eyestalk tissues at the same time point within the same biological replicates revealed no significant differences for *Clk*, *Tim, Cwo, Vri,* and *Dbt* (Fig. 14 and 15). Pitzschler (2018) had similar

findings for *Clk*, *Tim*, *Cwo*, and *Vri* but also for *E75*, *Per* and *Cry2* in krill held under laboratory controlled LD 12:12. The results of the present study suggest that in wild winter krill both tissues are equally important for the gene expression of detected genes and additionally for the expression of *Dbt*. However, for *Cyc*, *Sgg, Per*, *Cry2*, *E75,* and *Atpg* significant variations could be demonstrated between brain and eyestalks (Fig. 14 and 15), which is in contrast to Pitzschler (2018) who only found differences for *Cyc* and *Sgg*. For *Cyc*, one of six investigated time points, and for *Sgg,* two of six investigated time points indicated significant higher mRNA levels in brain and eyestalks. For *Per*, *Cry2*, and *Atpg*, three of six investigated time points, and for *E75* four of six investigated time points indicated significant higher mRNA expression levels in brain and eyestalks. Due to the fact that not all examined time points showed significant differences between the tissues, it is impossible to conclude in which of the investigated tissues gene expression is actually higher. Ultimately, the similar patterns of gene expression observed in both tissues supports the conclusion to use the whole head of krill in future investigations, also in order to prevent contaminations and to minimize other potential sources of error caused by tissues separation.

Putative co-regulation of clock genes between tissues

In this study, the relative mRNA maxima in the respective tissues were compared over time to identify putative co-regulation between brain and eyestalks in krill (Fig. 16). Mean expression levels of the core clock genes *Clk* and *Cyc* and the associated clock genes *Cwo* and *Sgg* showed two maxima at TP02 and TP06 shifted by 16 hours (Fig. 16, green). For *Clk,* maxima mean expression levels in brain were exhibited afterwards, shifted by 4 hours (TP03), while for the other clock genes maxima expression levels in brain were shifted by 16 hours (TP06). Maxima mean expression levels of core clock gene regulators *Per* and *Cry2* showed two maxima in brain at TP01 and TP06 shifted by 20 hours (Fig.16, green) and a maximum expression level in eyestalks shifted by 20 hours (TP06). The maxima mean expression levels of the regulator *Tim* and the associated clock gene *Dbt* in both tissues exhibited a shift of 24 hour (TP06) (Fig. 16, green, violet).

In general, nine out of ten clock genes displayed a general tendency for upregulation in the early night (TP06) in both tissues. This tendency for clock genes in krill was also observed in previous laboratory studies (Piccolin *et al.,* 2018a). This is remarkable and suggests that the daily patterns of expression might indeed have been synchronized to the photoperiod in the investigated krill, despite all difficulties related to the different light exposure which the krill may have experienced by

vertically moving in the water column. One hypothesis could be that an endogenous rhythm is present at the molecular level which might only require brief light pulses at specific times during the day in order to be entrained as already shown in other marine zooplankton (van Haren and Compton, 2013; Cohen *et al*., 2015; Cisewski and Strass, 2016; Häfker *et al*., 2017). In the context of DVM, these light pulses might influence the krill as they are ascending towards the surface around sunset. Those impulses might be sufficient to entrain the clock for the following 24 h, contributing to the regulation of the descent towards deeper layers before sunrise, and triggering the next ascent on the following day. Of course, it must be also noted that the TP06 has been collected with a time difference of 53.5 h compared to the previous time points and therefore it might be questionable whether the data for TP06 are representative.

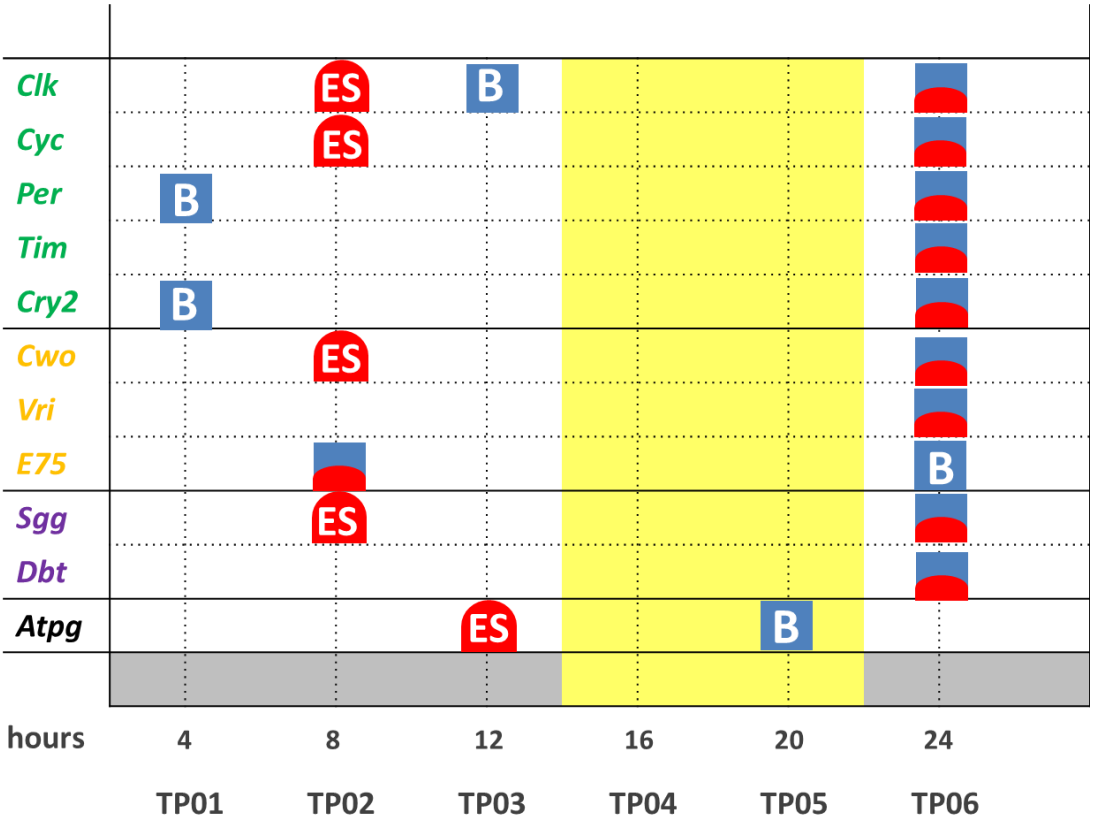

Figure 16: Schematic representation of potential co-regulation of clock genes over idealized 24 h cycle – Mean expression levels of *Clk, Cyc, Per, Tim, Cry2, Cwo, Vri, E75, Sgg, Dbt,* and *Atpg* were analyzed over 18 h +/- 6 hours to identify putative rhythmicity within a range of periods included between 12 h and 24 h in daily patterns of gene expression. We tested for this range of periods to ensure a detection of all rhythmic circadian behavior, including potential bimodal patterns with 12 h. 'Hours' indicates the distance towards the next repetition in hours (potential rhythmicity). TP = time point, displays the time point of sampling every 3.5 h in a time period of 24 h, except for TP06 (it was 53.5 h). Distances between TPs were idealized to 4 hours due to clarity. Blue squares with white 'B' illustrate highest NRQ levels in brain, red half round squares with white 'ES' illustrate maximum mean expression levels in eyestalks. Half blue/half red squares illustrate maximum expression levels for both tissues at the same time point. Values on y-axis cannot be equated with relative mRNA levels. Genes are grouped in core clock genes (green), associated clock genes (yellow), kinases (purple) and metabolic genes (black). Grey bar indicates dark phase at the sea surface, while yellow field indicates light phase at the sea surface.

4.4 Improvements and indications for future studies

In general, field studies of wild high-latitude species are always characterized by potential influences of environmental parameters (such as food availability, temperature, sea-ice cover, light regime), which, on the one hand makes it difficult to sample the animals and on the other incorporates very individual or special adaption regulations of the animals into the results. Thus, it may be advantageous to sample

wild krill in a 24 h cycle if possible and not to allow 53.5 h to elapse between TP05 and TP06, as in our case due to unfavorable weather conditions. Then again, however, it should be noted that this procedure was also done in approved previous field studies, where time points sampled on different days and locations were combined (Mazzotta *et al*., 2010; de Pittà *et al*., 2013). Nevertheless, to exclude influences of abrupt and extreme daily changes in high-latitude environments on to sampled krill, prolonged disruptions in sampling 24 h cycles together with changes in sampling locations should be avoided.

In general, studying gene expression of biologically diverse individuals requires the consideration of certain methodological limitations: i) gene expression underlies biological variation leading to differences in expression levels. The exclusion of presumed outliers should be carefully assessed to ensure not to exclude realistic data with individual biological variability (see also 2.10 Statistics). ii) potential specific differences in sexes. In this study, samples were not divided by sexes hence inter-sex differences in gene expression levels cannot be excluded.

Beyond others, this study contained the attempt to determine the optimal sampling tissue for future investigations in krill clock gene expression. Brain and eyestalks are known to contain circadian clock elements in crustacean (Strauss and Dircksen, 2010; Zhang *et al*., 2013) and therefore the potential differences in expression levels between krill brain and eyestalks were examined. The mRNA expression results of this study and the oscillation amplitudes which are comparable with other studies suggest that both tissues are suitable for an accurate determination of clock gene expression in krill. Taking into account the laborious dissection of the head into the individual tissue parts and the potential risk of contamination or damage to it, we recommend the use of the whole head for future clock gene expression studies. Furthermore, the knowledge about brain structures in krill should be expanded by examinations of different krill head tissues, because so far most studies are focused mostly on whole heads and eyestalks (Pittà *et al*., 2008; Mazotta *et al*., 2010; Teschke *et al*., 2011; Seear *et al*., 2012; de; Biscontin *et al*., 2017; Kilada *et al*., 2017 (eyestalks); Piccolin *et al*., 2018a, Höring *et al*., in prep publication I) and also by establishing more accurate ways (for example using FISH) where the peacemaker cells are located within the krill neural system (Zhao *et al*., 2003; Zhang *et al*., 2013; Kumar *et al.*, 2014).

5 Conclusion

Overall, knowledge of clock gene functions and regulations in high-latitude marine crustaceans, particularly in Antarctic krill, is very limited especially with regard to clock gene products, their distribution and their impact on oscillatory rhythmicity and chronobiological functions. Furthermore, studies of krill clock gene expression under natural winter conditions in the field are absent, thus this study provides initial insights into the regulatory clock work.

In the methodological part of the present study, the aim was to enhance the detection of potential oscillation patterns and to reduce gene expression variability by tissue-specific analyses of krill brain and eyestalks. Tissue-specific gene expressions showed 24 h rhythmic oscillation patterns in eyestalks for the clock gene *Tim* and for the metabolic gene *Atpg* as well as 16 h rhythmic oscillation for the clock genes *Cyc*. In addition, for the clock gene *Sgg* the tissue-specific gene expression displayed 24 h and 16 h rhythmic oscillation in both brain and eyestalks, respectively. It should be noted, that no significant differences between the tissue-specific amplitudes of oscillation were detected and moreover, tissue-specific results were comparable to previous gene expression findings from whole heads. Thus, for future studies using the entire head is recommended due to the indifferent amplitudes of oscillation between the examined brain and eyestalk tissues, but also regarding potential sources of error during the laborious separation of tissues.

In final conclusion, it can be stated that this study identified significant 24 h and 16 h oscillatory rhythms in the relative gene expression of three important clock genes, *Cyc*, *Sgg*, and *Tim*, as well as in the metabolic gene *Atpg* in brain and eyestalks of Antarctic krill in winter. Furthermore, nine of ten clock genes displayed a general tendency for upregulation in the early night in both tissues during low to even absent light regime. This leads to the assumption that an endogenous rhythm might be also active during winter controlling clock gene expression and output functions.

6 Outlook

With the identification of the transcriptome for the Antarctic key species *E*. *superba* (Hunt *et al*., 2017; Sales *et al*., 2017) a first molecular basis was established to enable more insights into chronobiological behavior and associated endogenous timing systems including contributions by certain clock genes at the transcriptional/translational level and at the neuroanatomical signal perception and transmission. Still, further detailed analyses of individual clock genes are required in order to characterize possible trigger mechanisms (*Zeitgeber*) on gene expression level as well as on protein level in order to determine a functional relationship within the krill endogenous clock system. One possibility might be to investigate disruptive effects on the circadian system by knock-out experiments of respective clock genes as already applied in insects (Bloch *et al*., 2003) or in marine crustaceans (Zhang *et al*., 2013). Knock-out cell lines do already exist for the terrestrial model organism *Drosophila*, but it is doubtful whether this will ever be possible for high-latitude krill. Future scientists must therefore be able to master challenges such as keeping krill in captivity, achieving focused reproduction of the animals, and promoting molecular genetic work on these small individuals. However, sampling wild krill in the field and working with them should be also pursued, as this might give a more realistic insight into the actual life circumstances of krill, which can be hardly reproduced in the laboratory (swarm behavior, DVM, food variability/intake behavior). In addition, techniques such as acoustic data or net catches for estimations concerning krill behavior, abundance or food availability, should be better linked in the future, using statistical analysis and ecological modelling (Tarling *et al*., 2017; Meyer *et al*., 2017; Reiss *et al*., 2017; Bernard *et al*., 2018).

Furthermore, the exact localization of clock neurons in krill should be detected which requires an integrative approach linking neuroanatomy, molecular physiology, and chronobiology. In *Drosophila*, antibodies against certain circadian clock proteins indicated the position of neurons containing respective genes and the gene expression within was important to generate circadian activity (Siwicki *et al.,* 1988; Zerr *et al*., 1990; Kaneko *et al.,* 2000; Helfrich-Förster *et al*., 2001). For a more holistic view of interaction, synchronization, and entrainment of clock genes in krill within and between tissues, the cellular distribution has to be defined. Therefore, it would be interesting to test already existing antibodies from *Drosophila* concerning suitability in Antarctic krill, as so far availability of krill specific antibodies is limited.

In summary, scientific work on the circadian clock system in krill, especially in wild Antarctic krill, will be an interesting challenge in the future. The connection of already existing and future data might allow a more holistic understanding of the

relationships between ecological and physiological processes, and how they are regulated by endogenous timing systems. The data collection of this study provides a first basic insight into clock gene expression patterns in late-winter wild krill, which can be used for further predictions regarding internal processes regulated by circadian mechanisms. Moreover, information about clock functioning in krill and their variable adaptive nature to high-latitude environments, should be further focused and investigated to predict the impact of environmental changes driven by climate change on the regulation of krill's life-cycle.

7 Acknowledgments

Hereby, I would like to thank my first supervisor Prof Dr Bettina Meyer for giving me the opportunity to do this exciting master's thesis topic in her ambitious working group and being supportive during my thesis. In particular, I would like to express my gratitude to Dr Fabio Piccolin for his enthusiasm, his patience, and his support. Moreover, I am more than thankful for his constructive criticism and his valuable comments to this thesis. In addition, I am very grateful that Dr Kim Last has agreed to by my second supervisor, although we only met once. Furthermore, special thanks to Dr Christian Reiss for answering all my questions regarding the krill samples and the circumstances of their procurement. Besides, my thanks also go to Katharina Michael for her suggestions and to Marvin Dörries for his helpful comments on this thesis.

Without my parents I would not be where I am now. I am very grateful for your everlasting support in all matters. Last but not least, special thanks from the bottom of my heart to all my friends for being there and your unswerving belief in me, especially to: M. L. Büsing, V. Vollmer, E. Linezki, and E. Zehren.

This thesis is dedicated to P. Bark and his curiosity.

8 Appendix

Determination of the optimal spike concentration for cDNA synthesis

Real-time quantitative PCR (qPCR) titration curves were applied to determine the optimal concentrations of the spikes for final chronobiologic analyses. A dilution series of the spike transcripts was prepared with different concentrations (5 ng, 500 pg (0.5 ng), 50 pg, 5 pg, 1.4 pg). The 4th dilution step (5 pg/µl) was diluted 1:3.5 instead of 1:10 to reduce the degree of dilution and therefore preserve the integrity of the spike RNA. The cDNA synthesis was accomplished by adding 1 µl of the different spike dilution steps (for cDNA synthesis protocol see 2.5 cDNA synthesis of eyestalks and brain samples). For each qPCR reaction, 5 µl of 1:5 diluted cDNA (4 ng/µl) were pipetted to 4 µl nuclease-free water, 1 µl primer mix (forward and reverse (360 µl, 20 x mix) of spike 1 and 2 or clock-gene), and 10 µl 2x TaqManTM Gene Expression Master Mix (Thermo Fisher Scientific, USA) to achieve a final reaction volume of 20 µl. Three technical replicates for each cDNA sample, no template controls (NTCs), and no reverse transcription controls (-RTs) were added on a 96-well reaction plate. In NTCs, the RNA template was replaced by nuclease-free water during cDNA synthesis to identify putative contaminations of the RT-qPCR master mix. Likewise, the enzyme reverse transcriptase was excluded in –RT controls during synthesis to inhibit the synthesis of cDNA in samples. qPCR 96-well plates were sealed, carefully vortexed, and briefly centrifuged. Thereafter, relative abundance of target RNAs was measured by the ViiATM 7 Real-Time PCR System (Thermo Fisher Scientific, USA). Reaction conditions were as follows: one cycle of stage 1 which included 50°C for 2 min and 95°C for 10 min, followed by 40 cycles of stage 2 which included 95°C for 15 s and 60°C for 1 min. After each qPCR run, results of NTCs and –RTs per plate were checked. Reliable results for NTCs should solely exhibit background noises or high Ct (cycle threshold) values as a result of primer-dimer formation. –RT controls allow the identification of DNA contamination, where genomic DNA gets amplified during qPCR runs and Ct values similar to those of samples may be detected. To analyze the samples as well as to compare between data obtained from different genes and qPCR runs, the baseline threshold for each qPCR run was set to 0.1. Due to the RT-qPCR results, 7.0 pg of spike 1 and spike 2 were utilized for further molecular biological analyses (Fig. 9A). This concentration displayed similar Ct values compared to test runs with known clock-genes (Fig. 9B) and consequently seemed appropriate.

Table 3: Primer efficiencies in tested brain tissues – Reaction efficiencies were calculated using the following formula: E = (10(-1/slope) -1) x 100.

Primer name	Slope	Amplification factor	R^2	Reaction efficiencies [%]
Clk_A	-3,3103	2,00	0,9089	100,49
Clk_B	-4,3833	1,69	0,9980	69,10
Cyc	-3,4442	1,95	0,9993	95,14
Atpg	-3,4631	1,94	0,9862	94,43
Per	-3,4000	1,97	0,9990	96,84
Tim_A	-3,5558	1,91	0,9697	91,09
Tim_B	-3,8451	1,82	0,9904	82,00
Cry2	-3,1924	2,06	0,9976	105,70
Cwo	-3,6588	1,88	0,9707	87,63
Vri	-3,5824	1,90	0,9882	90,17
Usp46	-3,3664	1,98	0,9826	98,18
Spike1	-3,4070	1,97	0,9993	96,57
Spike2	-2,8110	2,27	0,9803	126,85
E75	-3,6515	1,88	0,9902	87,87
Sgg	-4,5484	1,66	0,9930	65,90
Dbt	-4,1561	1,74	0,9375	74,02

Table 4: Primer efficiencies in tested eyestalk tissues – Reaction efficiencies were calculated using the following formula: E = (10(-1/slope) -1) x 100.

Primer name	Slope	Amplification factor	R^2	Reaction efficiencies [%]
Clk_A	-3,3106	2,00	0,9966	100,47
Clk_B	-4,2856	1,71	0,9979	71,14
Cyc	-3,5153	1,93	0,9987	92,52
Atpg	-3,1319	2,09	0,9881	108,59
Per	-3,2821	2,02	0,9987	101,69
Tim_A	-3,3900	1,97	0,9974	97,24
Tim_B	-3,2665	2,02	0,9910	102,37
Cry2	-3,0771	2,11	0,9455	111,34
Cwo	-3,5432	1,92	0,9927	91,53
Vri	-3,9398	1,79	0,9974	79,40
Usp46	-3,2292	2,04	0,9707	104,02
Spike1	-3,5418	1,92	0,9918	91,58
Spike2	-2,7609	2,30	0,9519	130,25
E75	-3,2588	2,03	0,9862	102,70
Sgg	-4,3727	1,69	0,9839	69,31
Dbt	-3,1439	2,08	0,9464	108,01

Table 5: Results of statistical RAIN analysis in brain implemented by R - Data were fit to a sinusoidal curve with the required period. *P*-values and the phases of the sinusoidal curve (amplitude of the oscillation is maximal) are shown in the table for each gene. *P*-values were corrected for multiple comparisons using the *false discovery method* (*fdr*) of Benjamini, Hochberg, and Yekutieli (Benjamini and Hochberg, 1995; Benjamini and Yekutieli, 2001) implemented within the RAIN package. Significant *p*-values are indicated in bold.

gene	*p*-value	phase	period	fdr-adjustment
Clk	0.892	12	12	
Cyc	0.871	24	24	
Atpg	0.270	20	24	
Per	0.926	4	20	
Tim	0.262	24	24	
Cry2	0.705	4	20	
Cwo	0.771	24	24	
Vri	0.778	24	24	
E75	0.899	8	16	
Sgg	**0.000062**	**24**	**24**	**0.0006864**
Dbt	0.126	24	24	

Table 6: Results of statistical RAIN Results of statistical RAIN analysis in brain implemented by R - Data were fit to a sinusoidal curve with the required period. *P*-values and the phases of the sinusoidal curve (amplitude of the oscillation is maximal) are shown in the table for each gene. *P*-values were corrected for multiple comparisons using the *false discovery method* (*fdr*) of Benjamini, Hochberg, and Yekutieli (Benjamini and Hochberg, 1995; Benjamini and Yekutieli, 2001) implemented within the RAIN package. Significant *p*-values are indicated in bold.

Clk	0.402	8	16	
Cyc	**0.017**	**8**	**16**	**0.048**
Atpg	**0.001**	**12**	**24**	**0.008**
Per	0.595	24	24	
Tim	**0.009**	**24**	**24**	**0.034**
Cry2	0.421	24	24	
Cwo	0.051	8	16	
Vri	0.124	24	24	
E75	0.135	8	20	
Sgg	**0.001**	**8**	**16**	**0.008**
Dbt	0.257	24	24	

Table 7: *P*-values of Mann-Whitney-Wilcoxon test - To compare the level of gene expression for each time point (TP) between eyestalk and brain tissues the Mann-Whitney-Wilcoxon test were used. Bold *p*-values were still significant after fdr adjustment.

	Atpg	Clk	Cry2	Cwo	Cyc	Dbt	E75	Per	Sgg	Tim	Vri
TP01	0.06954	0.06301	**0.02323**	0.2475	0.02881	0.03546	**0.0115**	**0.0115**	0.2176	0.3527	0.02323
TP02	**0.004135**	0.9682	**0.02218**	0.5954	0.8421	0.09472	**0.03041**	**0.01272**	**0.007621**	0.549	0.211
TP03	**0.002089**	0.02323	**0.005196**	1.00	**0.005196**	0.01258	**0.02323**	**0.00105**	0.2176	0.01469	0.03546
TP04	**0.02109**	0.2176	0.07526	0.7959	0.01854	0.06301	**0.01469**	0.08921	**0.008931**	0.2475	0.5787
TP05	0.315	0.7394	0.5288	0.8534	0.4813	0.06301	0.08921	0.6842	0.4813	0.1655	0.2176
TP06	0.62	0.62	0.1282	0.1098	0.8048	0.03788	0.09732	0.3176	0.3176	0.2593	0.3176

References

Aguzzi, J., Costa, C., Menesatti, P., García, J. A., Bahamon, N., Puig, P., & Sarda, F. (2011). Activity rhythms in the deep-sea: a chronobiological approach. *Frontiers in bioscience (Landmark edition)*, *16*, 131-150.

Allada, R., & Chung, B. Y. (2010). Circadian organization of behavior and physiology in Drosophila. *Annual review of physiology*, *72*, 605-624.

Andersen, C. L., Ledet-Jensen J., Ørntoft T.: Normalization of real-time quantitative RT-PCR data: a model based variance estimation approach to identify genes suited for normalization - applied to bladder- and colon-cancer data-sets. *Cancer Research*. 2004 (64): 5245-5250 *PubMed Supplementary data*

Aréchiga, H., & Rodríguez-Sosa, L. (2002). Distributed circadian rhythmicity in the crustacean nervous system. In *The crustacean nervous system* (pp. 113-122). Springer, Berlin, Heidelberg.

Aschoff, J. (1966). Circadian activity pattern with two peaks. Ecology 47(4):657–662.

Atkinson, A., Hill, S. L., Pakhomov, E. A., Siegel, V., Reiss, C. S., Loeb, V. J., ... & Sailley, S. F. (2019). Krill (Euphausia superba) distribution contracts southward during rapid regional warming. *Nature Climate Change*, *9*(2), 142.

Atkinson, A., Siegel, V., Pakhomov, E. A., Rothery, P., Loeb, V., Ross, R. M., ... & Tarling, G. A. (2008). Oceanic circumpolar habitats of Antarctic krill. *Marine Ecology Progress Series*, *362*, 1-23.

Atkinson, A., Siegel, V., Pakhomov, E., & Rothery, P. (2004). Long-term decline in krill stock and increase in salps within the Southern Ocean. *Nature*, *432*(7013), 100.

Atkinson, A., Meyer, B., Stuübing, D., Hagen, W., Schmidt, K., & Bathmann, U. V. (2002). Feeding and energy budgets of Antarctic krill Euphausia superba at the onset of winter—II. Juveniles and adults. *Limnology and Oceanography*, *47*(4), 953-966.

Bell-Pedersen, D., Cassone, V. M., Earnest, D. J., Golden, S. S., Hardin, P. E., Thomas, T. L., & Zoran, M. J. (2005). Circadian rhythms from multiple oscillators: lessons from diverse organisms. *Nature Reviews Genetics*, *6*(7), 544.

Benjamini, Y. & Hochberg, Y., 1995. Controlling the False Discovery Rate: a Practical and Powerful Approach to Multiple Testing. *Journal of the Royal Statistical Society. Series B (Methodological)*, 57(1), pp.289–300.

Benjamini, Y. & Yekutieli, D., 2001. The control of the false discovery rate in multiple testing under dependency. *The Annals of Statistics*, 29(4), pp.1165–1188.

Bernard, K. S., Gunther, L. A., Mahaffey, S. H., Qualls, K. M., Sugla, M., Saenz, B. T., ... & Handling editor: David Fields. (2018). The contribution of ice algae to the winter energy budget of juvenile Antarctic krill in years with contrasting sea ice conditions. *ICES Journal of Marine Science*, *76*(1), 206-216.

Biscontin, A., Frigato, E., Sales, G., Mazzotta, G. M., Teschke, M., De Pittà, C., ... & Bertolucci, C. (2016). The opsin repertoire of the Antarctic krill Euphausia superba. *Marine genomics*, *29*, 61-68.

Biscontin, A., Wallach, T., Sales, G., Grudziecki, A., Janke, L., Sartori, E., ... & Kramer, A. (2017). Functional characterization of the circadian clock in the Antarctic krill, Euphausia superba. *Scientific reports*, *7*(1), 17742.

Bloch, G., Solomon, S. M., Robinson, G. E., & Fahrbach, S. E. (2003). Patterns of PERIOD and pigment-dispersing hormone immunoreactivity in the brain of the European honeybee (Apis mellifera): age-and time-related plasticity. *Journal of Comparative Neurology*, *464*(3), 269-284.

Bollens, S. M., & Frost, B. W. (1991). Diel vertical migration in zooplankton: rapid individual response to predators. *Journal of Plankton Research*, *13*(6), 1359-1365.

Brierley, A. S. (2014). Diel vertical migration. *Current biology*, *24*(22), R1074-R1076.

Brown, M., Kawaguchi, S., Candy, S., Yoshida, T., Virtue, P., & Nicol, S. (2013). Long-term effect of photoperiod, temperature and feeding regimes on the respiration rates of Antarctic krill (Euphausia superba). *Open Journal of Marine Science*, *3*(2A), 40-51.

Brown, M., Kawaguchi, S., King, R., Virtue, P., & Nicol, S. (2010). Flexible adaptation of the seasonal krill maturity cycle in the laboratory. *Journal of plankton research*, *33*(5), 821-826.

Cavallari, N., Frigato, E., Vallone, D., Fröhlich, N., Lopez-Olmeda, J. F., Foà, A., ... & Foulkes, N. S. (2011). A blind circadian clock in cavefish reveals that opsins mediate peripheral clock photoreception. *PLoS biology*, *9*(9), e1001142.

Cisewski, B., & Strass, V. H. (2016). Acoustic insights into the zooplankton dynamics of the eastern Weddell Sea. *Progress in oceanography*, *144*, 62-92.

Cisewski, B., Strass, V. H., Rhein, M., & Krägefsky, S. (2010). Seasonal variation of diel vertical migration of zooplankton from ADCP backscatter time series data in the Lazarev Sea, Antarctica. *Deep Sea Research Part I: Oceanographic Research Papers*, *57*(1), 78-94.

Clarke, A., & Harris, C. M. (2003). Polar marine ecosystems: major threats and future change. *Environmental Conservation*, *30*(1), 1-25.

Cleary, A. C., Durbin, E. G., Casas, M. C., & Zhou, M. (2016). Winter distribution and size structure of Antarctic krill Euphausia superba populations in-shore along the West Antarctic Peninsula. *Marine Ecology Progress Series*, *552*, 115-129.

Cohen, J. H., Berge, J., Moline, M. A., Sørensen, A. J., Last, K., Falk-Petersen, S., ... & Cronin, H. (2015). Is ambient light during the high Arctic polar night sufficient to act as a visual cue for zooplankton?. *Plos One*, *10*(6), e0126247.

Cohen, J. H., & Forward, R. B. (2005). Diel vertical migration of the marine copepod Calanopia americana. I. Twilight DVM and its relationship to the diel light cycle. *Marine biology*, *147*(2), 387-398.

Cohen, J. H., & Forward Jr, R. B. (2009). Zooplankton diel vertical migration—a review of proximate control. In *Oceanography and marine biology*: An Annual Review 47:77–110. CRC press.

Curran, M. A., van Ommen, T. D., Morgan, V. I., Phillips, K. L., & Palmer, A. S. (2003). Ice core evidence for Antarctic sea ice decline since the 1950s. *Science*, *302*(5648), 1203-1206.

Dunlap, J. C. (1999). Molecular bases for circadian clocks. *Cell*, *96*(2), 271-290.

Frank, T. M., & Widder, E. A. (1999). Comparative study of the spectral sensitivities of mesopelagic crustaceans. *Journal of Comparative Physiology A*, *185*(3), 255-265.

Gaten, E., Tarling, G., Dowse, H., Kyriacou, C., & Rosato, E. (2008). Is vertical migration in Antarctic krill (Euphausia superba) influenced by an underlying circadian rhythm?. *Journal of genetics*, *87*(5), 473.

Gliwicz, M. Z. (1986). Predation and the evolution of vertical migration in zooplankton. *Nature*, *320*(6064), 746.

Häfker, N. S., Meyer, B., Last, K. S., Pond, D. W., Hüppe, L., & Teschke, M. (2017). Circadian clock involvement in zooplankton diel vertical migration. *Current Biology*, *27*(14), 2194-2201.

van Haren, H., & Compton, T. J. (2013). Diel vertical migration in deep sea plankton is finely tuned to latitudinal and seasonal day length. *PLoS One*, *8*(5), e64435.

Hardin, P. E. (2009). Molecular mechanisms of circadian timekeeping in Drosophila. *Sleep and Biological Rhythms*, *7*(4), 235-242.

Hays, G. C. (2003). A review of the adaptive significance and ecosystem consequences of zooplankton diel vertical migrations. In *Migrations and dispersal of marine organisms* (pp. 163-170). Springer, Dordrecht.

Helfrich-Förster, C., Winter, C., Hofbauer, A., Hall, J. C., & Stanewsky, R. (2001). The circadian clock of fruit flies is blind after elimination of all known photoreceptors. *Neuron*, *30*(1), 249-261.

Hellemans, J., Mortier, G., De Paepe, A., Speleman, F., Vandesompele, J. (2007). qBase relative quantification framework and software for management and automated analysis of real-time quantitative PCR data. *Genome biology*, 8(2), p.R19.

Hill, S. L., Phillips, T., & Atkinson, A. (2013). Potential climate change effects on the habitat of Antarctic krill in the Weddell quadrant of the Southern Ocean. *PloS one*, *8*(8), e72246.

Höring, F., Teschke, M., Suberg, L., Kawaguchi, S., & Meyer, B. (2018). Light regime affects the seasonal cycle of Antarctic krill (Euphausia superba): impacts on growth, feeding, lipid metabolism, and maturity. *Canadian Journal of Zoology*, *96*(11), 1203-1213.

Hunt, B. J., Özkaya, Ö., Davies, N. J., Gaten, E., Seear, P., Kyriacou, C. P., ... & Rosato, E. (2017). The Euphausia superba transcriptome database, Superba SE: An online, open resource for researchers. *Ecology and evolution*, *7*(16), 6060-6077.

Kaneko, M., Park, J. H., Cheng, Y., Hardin, P. E., & Hall, J. C. (2000). Disruption of synaptic transmission or clock-gene-product oscillations in circadian pacemaker cells of Drosophila cause abnormal behavioral rhythms. *Journal of neurobiology*, *43*(3), 207-233.

Kawaguchi, S., Yoshida, T., Finley, L., Cramp, P., & Nicol, S. (2006). The krill maturity cycle: a conceptual model of the seasonal cycle in Antarctic krill. *Polar Biology*, *30*(6), 689-698.

Kawaguchi, S., Finley, L. A., Jarman, S., Candy, S. G., Ross, R. M., Quetin, L. B., ... & Nicol, S. (2007). Male krill grow fast and die young. *Marine Ecology Progress Series*, *345*, 199-210.

Kawaguchi, S., King, R., Meijers, R., Osborn, J. E., Swadling, K. M., Ritz, D. A., & Nicol, S. (2010). An experimental aquarium for observing the schooling behaviour of Antarctic krill (Euphausia superba). *Deep Sea Research Part II: Topical Studies in Oceanography*, *57*(7-8), 683-692.

Kawaguchi, S., Ishida, A., King, R., Raymond, B., Waller, N., Constable, A., ... & Ishimatsu, A. (2013). Risk maps for Antarctic krill under projected Southern Ocean acidification. *Nature Climate Change*, *3*(9), 843.

Kilada, R., Reiss, C. S., Kawaguchi, S., King, R. A., Matsuda, T., & Ichii, T. (2017). Validation of band counts in eyestalks for the determination of age of Antarctic krill, Euphausia superba. *PloS one*, *12*(2), e0171773.

Kimes, P. (2018). sigclust2: sigclust2: Statistical Significance of Clustering. R package version 1.2.4.

Knox, G. A. (1984). The key role of krill in the ecosystem of the Southern Ocean with special reference to the Convention on the Conservation of Antarctic Marine Living Resources. *Ocean Management*, *9*(1-2), 113-156.

Kronfeld-Schor, N., Visser, M. E., Salis, L., & van Gils, J. A. (2017). Chronobiology of interspecific interactions in a changing world. *Philosophical Transactions of the Royal Society B: Biological Sciences*, *372*(1734), 20160248.

Kuhlman, S. J., Mackey, S. R., & Duffy, J. F. (2007, January). Biological Rhythms Workshop I: introduction to chronobiology. In *Cold Spring Harbor symposia on quantitative biology* (Vol. 72, pp. 1-6). Cold Spring Harbor Laboratory Press.

Kumar, S., Chen, D., Jang, C., Nall, A., Zheng, X., & Sehgal, A. (2014). An ecdysone-responsive nuclear receptor regulates circadian rhythms in Drosophila. *Nature communications*, *5*, 5697.

Lahiri, K., Vallone, D., Gondi, S. B., Santoriello, C., Dickmeis, T., & Foulkes, N. S. (2005). Temperature regulates transcription in the zebrafish circadian clock. *PLoS biology*, *3*(11), e351.

Last, K. S., Hobbs, L., Berge, J., Brierley, A. S., & Cottier, F. (2016). Moonlight drives ocean-scale mass vertical migration of zooplankton during the Arctic winter. *Current Biology*, *26*(2), 244-251.

Mackey, S. R. (2007, January). Biological Rhythms Workshop IA: molecular basis of rhythms generation. In *Cold Spring Harbor symposia on quantitative biology* (Vol. 72, pp. 7-19). Cold Spring Harbor Laboratory Press.

Matsumoto, A., Ukai-Tadenuma, M., Yamada, R. G., Houl, J., Uno, K. D., Kasukawa, T., ... & Hardin, P. E. (2007). A functional genomics strategy reveals clockwork orange as a transcriptional regulator in the Drosophila circadian clock. *Genes & development*, *21*(13), 1687-1700.

Mauchline, J., & Fisher, L. R. (1969). Advances in marine biology. Vol. 7. *The biology of euphausiids. New York*.

Mauchline, J., (1980) Measurement of body length of *Euphausia superba* Dana. BIOMASS Handbook, No 4:9 pp.

Mazzotta, G. M., De Pittà, C., Benna, C., Tosatto, S. C., Lanfranchi, G., Bertolucci, C., & Costa, R. (2010). A cry from the krill. *Chronobiology international*, *27*(3), 425-445.

Meredith, M. P., & King, J. C. (2005). Rapid climate change in the ocean west of the Antarctic Peninsula during the second half of the 20th century. *Geophysical Research Letters*, *32*(19).

Merlin, C., Gegear, R. J., & Reppert, S. M. (2009). Antennal circadian clocks coordinate sun compass orientation in migratory monarch butterflies. *Science*, *325*(5948), 1700-1704.

Meyer, B., Freier, U., Grimm, V., Groeneveld, J., Hunt, B. P., Kerwath, S., ... & Melbourne-Thomas, J. (2017). The winter pack-ice zone provides a sheltered but food-poor habitat for larval Antarctic krill. *Nature ecology & evolution*, *1*(12), 1853.

Meyer, B. (2012). The overwintering of Antarctic krill, Euphausia superba, from an ecophysiological perspective. *Polar Biology*, *35*(1), 15-37.

Meyer, B., Auerswald, L., Siegel, V., Spahić, S., Pape, C., Fach, B. A., ... & Fuentes, V. (2010). Seasonal variation in body composition, metabolic activity, feeding, and growth of adult krill Euphausia superba in the Lazarev Sea. *Marine Ecology Progress Series*, *398*, 1-18.

Murphy, E. J., Watkins, J. L., Trathan, P. N., Reid, K., Meredith, M. P., Thorpe, S. E., ... & Forcada, J. (2006). Spatial and temporal operation of the Scotia Sea ecosystem: a review of large-scale links in a krill centred food web. *Philosophical Transactions of the Royal Society B: Biological Sciences*, *362*(1477), 113-148.

Neuwirth, E. (2014). RColorBrewer: ColorBrewer Palettes. R package version 1.1-2.https://CRAN.R-project.org/package=RColorBrewer

Nicol, S. (1994). Antarctic krill—changing perceptions of its role in the Antarctic ecosystem. In *Antarctic Science* (pp. 144-166). Springer, Berlin, Heidelberg.

Nicol, S., Foster, J., & Kawaguchi, S. (2012). The fishery for Antarctic krill–recent developments. *Fish and Fisheries*, *13*(1), 30-40.

Piccolin, F., Meyer, B., Biscontin, A., De Pittà, C., Kawaguchi, S., & Teschke, M. (2018a). Photoperiodic modulation of circadian functions in Antarctic krill Euphausia superba Dana, 1850 (Euphausiacea). *Journal of Crustacean Biology*, *38*(6), 707-715.

Piccolin, F., Suberg, L., King, R., Kawaguchi, S., Meyer, B., & Teschke, M. (2018b). The seasonal metabolic activity cycle of Antarctic krill (Euphausia superba): evidence for a role of photoperiod in the regulation of endogenous rhythmicity. *Frontiers in physiology*, *9*, 1715.

Piccolin, F., Pitzschler, L., Biscontin, A., Kawaguchi, S., Teschke, M., Meyer, B. (in prep.) Endogenous regulation of DVM in Antarctic krill (*Euphausia superba*) and its link with photoperiod and circadian clock activity

De Pitta, C., Biscontin, A., Albiero, A., Sales, G., Millino, C., Mazzotta, G. M., ... & Costa, R. (2013). The Antarctic krill Euphausia superba shows diurnal cycles of transcription under natural conditions. *PLoS One*, *8*(7), e68652.

Pitzschler, L. (2018). *Daily patterns of clock gene expression in Antarctic krill, Euphausia superba, under a 12h: 12h light: dark cycle in the laboratory* (Master's thesis, University of Oldenburg).

Quetin, L. B., & Ross, R. M. (1991). Behavioral and physiological characteristics of the Antarctic krill, Euphausia superba. *American Zoologist*, *31*(1), 49-63.

Ramakers, C., Ruijter, J. M., Deprez, R. H. L., & Moorman, A. F. (2003). Assumption-free analysis of quantitative real-time polymerase chain reaction (PCR) data. *Neuroscience letters*, *339*(1), 62-66.

Reiss, C. S., Cossio, A. M., Loeb, V., & Demer, D. A. (2008). Variations in the biomass of Antarctic krill (Euphausia superba) around the South Shetland Islands, 1996–2006. *ICES Journal of Marine Science*, *65*(4), 497-508.

Reiss, C. S., Cossio, A., Santora, J. A., Dietrich, K. S., Murray, A., Mitchell, B. G., ... & Watters, G. M. (2017). Overwinter habitat selection by Antarctic krill under varying sea-ice conditions: implications for top predators and fishery management. *Marine Ecology Progress Series*, *568*, 1-16.

Reppert, S. M. (2007, January). The ancestral circadian clock of monarch butterflies: role in time-compensated sun compass orientation. In *Cold Spring Harbor symposia on quantitative biology* (Vol. 72, pp. 113-118). Cold Spring Harbor Laboratory Press.

Rosner, B. (1983), "Percentage Points for a Generalized ESD Many-Outlier Procedure," *Technometrics*, Vol. 25, No. 2, pp. 165-172.

Rubin, E. B., Shemesh, Y., Cohen, M., Elgavish, S., Robertson, H. M., & Bloch, G. (2006). Molecular and phylogenetic analyses reveal mammalian-like clockwork in the honey bee (Apis mellifera) and shed new light on the molecular evolution of the circadian clock. *Genome research*, *16*(11), 1352-1365.

Rutledge, R. G., & Cote, C. (2003). Mathematics of quantitative kinetic PCR and the application of standard curves. *Nucleic acids research*, *31*(16), e93-e93.

Sales, G., Deagle, B.E., Calura, E., Martini, P., Biscontin, A., De Pittà, C., Kawaguchi, S., Romualdi, C., Meyer, B., Costa, R., Jarman, S. (2017). KrillDB: A de novo transcriptome database for the Antarctic krill (Euphausia superba). *PLoS ONE*, 12(2), pp.1–12.

Sbragaglia, V., Lamanna, F., Mat, AM., Rotllant, G., Joly, S., Ketmaier, V., ... & Aguzzi, J. (2015). Identification, characterization, and diel pattern of expression of canonical clock genes in Nephrops norvegicus (Crustacea: Decapoda) eyestalk. *PLoS One*, *10*(11), e0141893.

Schiermeier, Q. (2010). Ecologists fear Antarctic krill crisis.

Seear, P. J., Goodall-Copestake, W. P., Fleming, A. H., Rosato, E., & Tarling, G. A. (2012). Seasonal and spatial influences on gene expression in Antarctic krill Euphausia superba. *Marine Ecology Progress Series*, *467*, 61-75.

Seear, P., Tarling, G. A., Teschke, M., Meyer, B., Thorne, M. A., Clark, M. S., ... & Rosato, E. (2009). Effects of simulated light regimes on gene expression in Antarctic krill (Euphausia superba Dana). *Journal of Experimental Marine Biology and Ecology*, *381*(1), 57-64.

Siegel, V. (2000). Krill (Euphausiacea) demography and variability in abundance and distribution. *Canadian Journal of Fisheries and Aquatic Sciences*, *57*(S3), 151-167.

Siegel, V. (2005). Distribution and population dynamics of Euphausia superba: summary of recent findings. *Polar Biology*, *29*(1), 1-22.

Siegel, V. (Ed.). (2016). *Biology and ecology of Antarctic krill*. Springer.

Siwicki, K. K., Eastman, C., Petersen, G., Rosbash, M., & Hall, J. C. (1988). Antibodies to the period gene product of Drosophila reveal diverse tissue distribution and rhythmic changes in the visual system. *Neuron*, *1*(2), 141-150.

Smetacek, V., & Nicol, S. (2005). Polar ocean ecosystems in a changing world. *Nature*, *437*(7057), 362.

Smith, D. A., Hofmann, E. E., Klinck, J. M., & Lascara, C. M. (1999). Hydrography and circulation of the west Antarctic Peninsula continental shelf. *Deep Sea Research Part I: Oceanographic Research Papers*, *46*(6), 925-949.

Sourisseau, M., Simard, Y., & Saucier, F. J. (2008). Krill diel vertical migration fine dynamics, nocturnal overturns, and their roles for aggregation in stratified flows. *Canadian Journal of Fisheries and Aquatic Sciences*, *65*(4), 574-587.

Strauss, J., & Dircksen, H. (2010). Circadian clocks in crustaceans: identified neuronal and cellular systems. *Frontiers in bioscience*, *15*(1), 1040-1074.

Tarling, G. A., & Thorpe, S. E. (2017). Oceanic swarms of Antarctic krill perform satiation sinking. *Proceedings of the Royal Society B: Biological Sciences*, *284*(1869), 20172015.

Teschke, M., Wendt, S., Kawaguchi, S., Kramer, A., & Meyer, B. (2011). A circadian clock in Antarctic krill: an endogenous timing system governs metabolic output rhythms in the euphausid species *Euphausia superba*. *PLoS One*, *6*(10), e26090

Teschke, M., Kawaguchi, S., & Meyer, B. (2008). Effects of simulated light regimes on maturity and body composition of Antarctic krill, Euphausia superba. *Marine biology*, *154*(2), 315-324.

Teschke, M., Kawaguchi, S., & Meyer, B. (2007). Simulated light regimes affect feeding and metabolism of Antarctic krill, Euphausia superba. *Limnology and oceanography*, *52*(3), 1046-1054.

Tessmar-Raible, K., Raible, F., & Arboleda, E. (2011). Another place, another timer: marine species and the rhythms of life. *Bioessays*, *33*(3), 165-172.

Thaben, P.F. & Westermark, P.O. (2014). Detecting rhythms in time series with rain. *Journal of Biological Rhythms*, 29(6), pp.391–400.

Tomioka, K., & Matsumoto, A. (2015). Circadian molecular clockworks in non-model insects. *Current Opinion in Insect Science*, *7*, 58-64.

Torres, J. J., Aarset, A. V., Donnelly, J., Hopkins, T. L., Lancraft, T. M., & Ainley, D. G. (1994). Metabolism of Antarctic micronektonic Crustacea as a function of depth of occurrence and season. *Marine ecology-progress series*, *113*(3), 207.

Tou, J. C., Jaczynski, J., & Chen, Y. C. (2007). Krill for human consumption: nutritional value and potential health benefits. *Nutrition reviews*, *65*(2), 63-77.

Warnes, G. R., Bolker, B., Bonebakker, L., Gentleman, R., Huber, W., Liaw, A., Lumley, T., Maechler, M., Magnusson, A., Moeller, S., Schwartz, M. and Venables, B. (2019). gplots: Various R Programming Tools for Plotting Data. R package version 3.0.1.1.https://CRAN.R-project.org/package=gplots

Williams CT, Barnes BM, Buck CL (2015). Persistence, entrainment, and function of circadian rhythms in polar vertebrates. Physiology 30(2):86–96.

Yoshitomi, B., Aoki, M., & Oshima, S. I. (2007). Effect of total replacement of dietary fish meal by low fluoride krill (Euphausia superba) meal on growth performance of rainbow trout (Oncorhynchus mykiss) in fresh water. *Aquaculture*, *266*(1-4), 219-225.

Zantke, J., Ishikawa-Fujiwara, T., Arboleda, E., Lohs, C., Schipany, K., Hallay, N., ... & Tessmar-Raible, K. (2013). Circadian and circalunar clock interactions in a marine annelid. *Cell reports*, *5*(1), 99-113.

Zerr, D. M., Hall, J. C., Rosbash, M., & Siwicki, K. K. (1990). Circadian fluctuations of period protein immunoreactivity in the CNS and the visual system of Drosophila. *Journal of Neuroscience*, *10*(8), 2749-2762.

Zhang, L., Hastings, M. H., Green, E. W., Tauber, E., Sladek, M., Webster, S. G., ... & Wilcockson, D. C. (2013). Dissociation of circadian and circatidal timekeeping in the marine crustacean Eurydice pulchra. *Current Biology*, *23*(19), 1863-1873.

Zhao, J., Kilman, V. L., Keegan, K. P., Peng, Y., Emery, P., Rosbash, M., & Allada, R. (2003). Drosophila clock can generate ectopic circadian clocks. *Cell*, *113*(6), 755-766.

Zhou, M., & Dorland, R. D. (2004). Aggregation and vertical migration behavior of Euphausia superba. *Deep Sea Research Part II: Topical Studies in Oceanography*, *51*(17-19), 2119-2137.

Zhu, H., Sauman, I., Yuan, Q., Casselman, A., Emery-Le, M., Emery, P., & Reppert, S. M. (2008). Cryptochromes define a novel circadian clock mechanism in monarch butterflies that may underlie sun compass navigation. *PLoS biology*, *6*(1), e4.

Statutory declaration

I hereby certify that I have written the present master thesis entitled

Clock gene expression patterns in brain and eyestalk tissue of freshly caught Antarctic krill, *Euphausia superba*, during winter

on my own and independently and that I have used no other than the indicated sources and means. Any thoughts or quotations which were inferred from these sources, either verbatim or as a paraphrase, have been marked as such. Furthermore, I assure that I have followed the general principles of scientific work and publication as defined in the guidelines of good scientific practice of the Carl von Ossietzky University of Oldenburg.

Oldenburg, September 9, 2019 *Constanze Bark*